

AD-764 709

DEVELOPMENT AND CONSTRUCTION OF A LINE-
TUNABLE FUNDAMENTAL-MODE PULSED HF/DF
LASER

Dietmar E. Rothe

Lumonics Research Limited

Prepared for:

Rome Air Development Center
Advanced Research Projects Agency

April 1973

DISTRIBUTED BY:

NTIS

National Technical Information Service
U. S. DEPARTMENT OF COMMERCE
5285 Port Royal Road, Springfield Va. 22151

RADC-TR-73-173
Final Technical Report
April 1973



AD 764709

DEVELOPMENT AND CONSTRUCTION OF A LINE-TUNABLE
FUNDAMENTAL-MODE PULSED HF/DF LASER

Lumonics Research Ltd.

Sponsored by
Defense Advanced Research Projects Agency
ARPA Order No. 1279

Approved for public release;
distribution unlimited.

The views and conclusions contained in this document are those of the authors and should not be interpreted as necessarily representing the official policies, either expressed or implied, of the Defense Advanced Research Projects Agency or the U. S. Government.

Reproduced by
NATIONAL TECHNICAL
INFORMATION SERVICE
U S Department of Commerce
Springfield VA 22151

Rome Air Development Center
Air Force Systems Command
Griffiss Air Force Base, New York



DEVELOPMENT AND CONSTRUCTION OF A LINE-TUNABLE
FUNDAMENTAL-MODE PULSED HF/DF LASER

Dietmar E. Rothe

Contractor: Lumonics Research Ltd.
Contract Number: F30602-72-C-0394
Effective Date of Contract: 31 May 1972
Contract Expiration Date; 31 October 1972
Amount of Contract: \$39,142.00
Program Code Number: 1E20

Principal Investigator: Dietmar E. Rothe
Phone: 613 225-1606

Project Engineer: James W. Cusack
Phone: 315 330-3145

ACCESSION for	
NTIS	White Section <input checked="" type="checkbox"/>
GPC	Defi Section <input type="checkbox"/>
UNCLASSIFIED	<input type="checkbox"/>
JUSTIFICATION	
BY	
DISTRIBUTION/AVAILABILITY CODES	
Dist.	Avail. and/or SPECIAL
A	

Approved for public release;
distribution unlimited.

This research was supported by the
Defense Advanced Research Projects
Agency of the Department of Defense
and was monitored by James W. Cusack
RADC (OCSE), GAFB, NY 13441 under
Contract F30602-72-C-0394.

UNCLASSIFIED

Security Classification

DOCUMENT CONTROL DATA - R & D

(Security classification of title, body of abstract and indexing annotation must be entered when the overall report is classified)

1. ORIGINATING ACTIVITY (Corporate author) Lumonics Research Ltd 1755 Woodward Drive Ottawa 5, Canada		2a. REPORT SECURITY CLASSIFICATION Unclassified	
		2b. N/A	
3. REPORT TITLE Development and Construction of a Line - Tunable Pulsed HF/DF Laser			
4. DESCRIPTIVE NOTES (Type of report and inclusive dates) Final Report 31 Oct 72 - 31 Apr 73			
5. AUTHOR(S) (First name, middle initial, last name) Dietmar E Rothe			
6. REPORT DATE April 73		7a. TOTAL NO. OF PAGES 72 78	7b. NO. OF REFS 24
8a. CONTRACT OR GRANT NO. F30602-72-C-0394		9a. ORIGINATOR'S REPORT NUMBER(S) None	
b. PROJECT NO.		9b. OTHER REPORT NO(S) (Any other numbers that may be assigned this report) RADC-TR-73-173	
c.			
d.			
10. DISTRIBUTION STATEMENT Approved for public release; distribution unlimited			
11. SUPPLEMENTARY NOTES Monitored by James W. Cusack RADC/OCSE Griffiss AFB, NY 13440		12. SPONSORING MILITARY ACTIVITY Advanced Research Projects Agency 1400 Wilson Blvd. Arlington, VA 22209	
13. ABSTRACT This report describes a development program for the construction of a line-tunable single-mode pulsed TE-laser*, suitable for use with both HF and DF. Experiments performed with a prototype, aimed at suppression of the superradiant background, indicated that it was not possible to lower the optical gain significantly without adversely affecting the tuned pulse energies and the pulse-to-pulse energy reproducibility. In the final laser configuration the superradiant background was removed with an in-line filter. The beam divergence was minimized by employing a fundamental-mode unstable resonator and a beam expander which produced a 10 cm diameter beam with a divergence of less than 0.2 milliradian in the far field. The test program and the construction and performance of this laser system are discussed in detail herein. *TE refers to laser excitation in a pulsed transverse electric discharge.			

DD FORM 1473
1 NOV 65

UNCLASSIFIED

Security Classification

1a

UNCLASSIFIED

Security Classification

14 KEY WORDS	LINK A		LINK B		LINK C	
	ROLE	WT	ROLE	WT	ROLE	WT
Pulsed Chemical HF/DF Laser						
TE-Laser						
Spectral Tuning						
Unstable Resonator						
Single Fundamental Mode						
Superradiance						
Gain Suppression						
Pulse Shapes						
Tuned Spectral Output						
Intra-Cavity Grating						
Monochromator						
Beam Expander						

UNCLASSIFIED

Security Classification

1/6

RADC-TR-73-173
Final Technical Report
April 1973



DEVELOPMENT AND CONSTRUCTION OF A LINE-TUNABLE
FUNDAMENTAL-MODE PULSED HF/DF LASER

Lumonics Research Ltd.

Sponsored by
Defense Advanced Research Projects Agency
ARPA Order No. 1279

Approved for public release;
distribution unlimited.

The views and conclusions contained in this document are those of the authors and should not be interpreted as necessarily representing the official policies, either expressed or implied, of the Defense Advanced Research Projects Agency or the U. S. Government.

Rome Air Development Center
Air Force Systems Command
Griffiss Air Force Base, New York

PUBLICATION REVIEW

This technical report has been reviewed and is approved.


RADC Project Engineer

LIST OF CONTENTS

		<u>Page</u>
I	ABSTRACT	1
II	INTRODUCTION	2
	a. History	2
	b. Program Goals	3
III	GENERAL CHARACTERISTICS OF PULSED HF/DF LASERS	5
IV	SPECTRAL TUNING EXPERIMENTS	11
V	DESCRIPTION OF LASER CONFIGURATION	19
	a. Electrodes and Discharge Circuit	19
	b. Gas Flow and Controls	20
	c. Optical Design	22
VI	PERFORMANCE SPECIFICATIONS OF DELIVERED SYSTEM	28
VII	CONCLUSIONS AND SUGGESTIONS FOR FUTURE DEVELOPMENT	31
VIII	REFERENCES	32
IX	FIGURES	35
X	APPENDIX - System Safety Analysis	

LIST OF FIGURES

- FIGURE 1 HF LASER POWER AS A FUNCTION OF PROPANE PERCENTAGE
- FIGURE 2 HF LASER POWER AS A FUNCTION OF GAS PRESSURE AT
CONSTANT FLOW VELOCITY AND CONSTANT COMPOSITION
- FIGURE 3 THE EFFECT ON THE HF LASER POWER OF THE ADDITION
OF HELIUM TO THE GAS MIXTURE
- FIGURE 4 OUTPUT POWER AND EFFICIENCY AS FUNCTION OF
CAPACITOR SIZE (PULSE WIDTH) AT 35 KV
- FIGURE 5 HF LASER POWER AS A FUNCTION OF FLOW VELOCITY
AT CONSTANT PRESSURE AND COMPOSITION
- FIGURE 6 HF-LASER OPTICAL PULSE SHAPES OBTAINED WITH
PHOTON DRAG
- FIGURE 7 LASER DISCHARGE CIRCUIT
- FIGURE 8 HF LASER OUTPUT SCANNED WITH INTRA-CAVITY GRATING
(P = 45 TORR)
- FIGURE 9 HF LASER OUTPUT SCANNED WITH INTRA-CAVITY GRATING
(P = 550 TORR)
- FIGURE 10 HF-SPECTRUM OF UNTUNED LASER EMISSION SCANNED
WITH EXTERNAL SPECTROMETER (P = 45 TORR)
- FIGURE 11 HF-SPECTRUM OF UNTUNED LASER EMISSION SCANNED WITH
EXTERNAL SPECTROMETER (P = 580 TORR)
- FIGURE 12 DF LASER OUTPUT SCANNED WITH INTRA-CAVITY GRATING
(P = 45 TORR)
- FIGURE 13 PULSE ENERGY VARIATION OF LASER OUTPUT TUNED TO HF-P₁(7)
LINE
- FIGURE 14 ENERGY VARIATION OF TUNED LASER OUTPUT AT 500 TORR
(WITH HF)
- FIGURE 15 OPTICAL PULSE SHAPES OF HF LASER (P = 45 TORR)

- FIGURE 16 OPTICAL PULSE SHAPES OF HF LASER ($P = 550$ TORR)
- FIGURE 17 PULSE-TO-PULSE VARIATION OF $P_1(7)$ LINE (HF)
AT 550 TORR
- FIGURE 18 LASER DISCHARGE SECTION
- FIGURE 19 GAS FLOW SYSTEM
- FIGURE 20 LASER BEAM OPTICS
- FIGURE 21 HF/DF LASER SYSTEM
- FIGURE 22 GRATING MOUNT AND DRIVE
- FIGURE 23 CROSS-SECTIONS OF THE OUTPUT BEAM FROM THE UNSTABLE
CAVITY FOR TWO DIFFERENT ELECTRODE SHAPES
- FIGURE 24 NEAR-FIELD BEAM PROFILE 50 M FROM LASER
- FIGURE 25 ENERGY DISTRIBUTION IN THE CENTRAL SPOT OF
FAR-FIELD BEAM (FAST RECORDING CIRCUIT)
- FIGURE 26 ENERGY DISTRIBUTION IN THE CENTRAL SPOT OF
FAR-FIELD BEAM (INTEGRATING CIRCUIT)

ACKNOWLEDGEMENTS

This development program was supported by the Advanced Research Projects Agency and by the Air Force Systems Command, Rome Air Development Center, Griffiss Air Force Base, New York under Contract No. F30602-72-C-0394 and was monitored by Messrs. James W. Cusack and Ray Urtz of RADC-GAFB.

The author wishes to acknowledge the helpful suggestions received from Drs. George H. Kimbell and Jacques Gilbert of the Canadian Defence Research Establishment at Valcartier, Quebec and the many useful discussions with Dr. John A. Nilson and Mr. Terry R. Schein of the Lumonics Research Staff. Special thanks are due to Dr. George A. Dobrowolski of the Canadian National Research Council for helping out with the design and application of several special dielectric coatings for the optics of this laser system.

I ABSTRACT

This report describes a development program for the construction of a line-tunable single-mode pulsed TE-laser*, suitable for use with both HF and DF. Experiments performed with a prototype, aimed at suppression of the superradiant background, indicated that it was not possible to lower the optical gain significantly without adversely affecting the tuned pulse energies and the pulse-to-pulse energy reproducibility.

In the final laser configuration the superradiant background was removed with an in-line filter. The beam divergence was minimized by employing a fundamental-mode unstable resonator and a beam expander which produced a 10 cm diameter beam with a divergence of less than 0.2 milliradian in the far field.

The test program and the construction and performance of this laser system are discussed in detail herein.

*TE refers to laser excitation in a pulsed transverse electric discharge.

II INTRODUCTION

a. History

The possibility of utilizing the energy release of an exothermic chemical reaction to produce a vibrational population inversion suitable for laser action was discussed by Polanyi¹ in 1961. The first such chemical hydrogen halide laser was subsequently demonstrated by Kasper and Pimentel² in 1965. In their work, amplified stimulated emission was obtained from vibrationally excited HCl molecules produced in a chemical reaction which was initiated by flash photolysis of a gas mixture containing hydrogen and chlorine. Chemically pumped laser transitions in HF were first reported in 1967 by Deutsch³ in a pulsed longitudinal electric discharge. In the same year a pulsed HF laser was also described by Kompa and Pimentel⁴.

Electric-discharge initiated chemical HF and DF lasers have since been studied and perfected by several investigators⁵⁻²⁰ employing various combinations of F donor molecules such as NF_3 , CF_4 , MoF_6 , UF_6 , $\text{C Cl}_2\text{F}_2$ etc. and hydrogen-containing compounds such as H_2 , C_2H_6 , C_3H_8 , C_4H_{10} , HI , HBr , gasoline etc.

Relatively high electric energy-conversion efficiencies (1 to 5%), comparable with those of pulsed CO_2 lasers, have recently been obtained for HF lasers by employing transverse discharge techniques.⁸⁻²⁰ Highest pulse energies have been obtained when SF_6 was used in combination with H_2 or with ethane, propane or butane.

Temporal and spectral characteristics of the optical output pulse have been studied for transverse discharge lasers employing resistively loaded pins by Jacobson and Kimbell^{8, 9, 10}, Green and Lin¹¹, Wood et al.^{12, 13}, Marcus and Carbone^{14, 15}, Deutsch¹⁶ and Pummer and Kompa¹⁷.

More recently, extended electrodes and double-discharge techniques were used at Lumonics¹⁸ and by Wenzel and Arnold¹⁹ and Jacobson and Kimbell²⁰ to improve further the efficiency and pulse energy of such lasers.

b. Program Goals

The research and development described herein was necessary for generating the decisions required for the design and construction of a pulsed HF/DF TE-laser system, which could meet simultaneously the following requirements:

1. The laser was to be readily line tunable over all available HF and DF lines, with the spectral purity of the tuned output being better than 98 per cent.
2. The average optical power on dominant spectral lines (at pulse repetition rates between one and ten pulses per second) was to be larger than 10 milliwatt.
3. Pulse energy variation was to be less than ± 2 per cent.
4. The laser was to operate in the fundamental transverse mode, and the beam divergence was to be approximately 0.1 mrad in the far field.

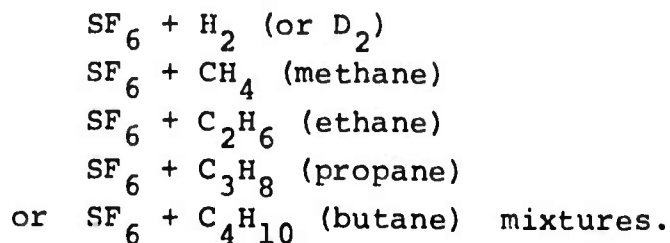
At the beginning of the development program these specifications were beyond the state-of-the-art of HF lasers, even though any one or two of these requirements could possibly have been met by an upgraded version of a standard Lumonics HF/DF laser system.

The major stumbling block, which prevents the attainment of high spectral purity and single-mode operation with low beam divergence, is the extremely high gain of all electrically initiated chemical HF lasers. In fact, such lasers have been observed ^{5, 14, 15} to be superradiant over an active length as short as one centimeter. Under these conditions it is not possible to control the output mode and spectral purity with the cavity reflectors. A major part of the development effort consisted, therefore, of a search for techniques which would reduce the optical gain and suppress the superradiance without unduly sacrificing pulse energy.

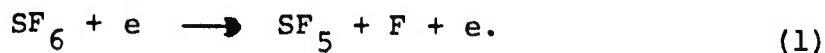
Characteristics of a typical pulse-initiated HF laser are outlined in Section III. Details of the development program are given in Section IV, and the resulting laser design and performance are described in Sections V and VI of this report.

III GENERAL CHARACTERISTICS OF PULSED HF/DF LASERS

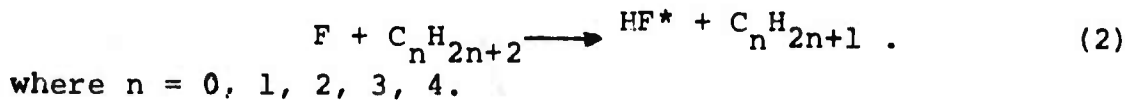
Apart from its compact design, the transverse electrically pulsed HF/DF laser has the advantage over other chemical HF lasers insofar that easily available, non-corrosive and non-toxic gases can be used as fuel. In addition, the exhaust gases contain only relatively small amounts of HF (or DF), simplifying the disposal problem. Best performance characteristics have been obtained with



In the operation of an electrically initiated HF laser, the function of the glow discharge is to dissociate a sufficient number of SF_6 molecules, i.e.



The free fluorine atoms then react with the hydrocarbon molecules to produce vibrationally excited HF atoms via the reaction



The energy release in this reaction which is available for vibrational excitation is 31.6 k cal/mole for H_2 or D_2 and is 32, 37, 40 and 43 k cal/mole for methane, ethane, propane and butane, respectively. The energies required to excite the first four vibrational states (above the ground state) of HF and DF are:

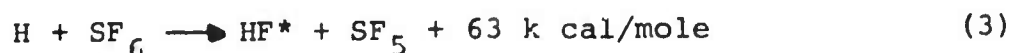
V	HF*	DF**
1	11.3 k. cal/mole	8.3 k cal/mole
2	22.2	16.3
3	32.5	24.0
4	42.4	31.5

* from Ref. 21

** estimated from wavelengths tabulated in Ref. 3

With ethane and propane the energy liberated is sufficient to populate the first three vibrationally excited states of HF. With butane the $v = 4$ state may also be excited; however, no $v = 4 \rightarrow 3$ transitions have yet been observed. When hydrogen or methane are used in combination with SF_6 , the $v = 3$ state of HF may only be excited if sufficient thermal energy is available from the gas discharge to supplement the chemical energy release. That this is indeed the case, is supported by the fact that strong laser action can be produced in the $v = 3 \rightarrow 2$ transition band with hydrogen^{10-13,18,20} or methane²⁰. Similarly, one would expect lasing to occur on the $v = 4 \rightarrow 3$ band of DF when SF_6 and D_2 are employed as fuel. However, P_4 lines have so far only been observed by Wood and Chang¹³ and were not seen in the laser described herein.

The complimentary process of reaction (2) involving H atoms produced in the discharge (or by reaction 2 if H_2 is used) also takes place, i.e.



Even though the exothermicity of this reaction is higher than that of process (2), this reaction is too slow to contribute significantly to the gain buildup in the laser.

For efficient operation of the laser, the HF formed in the discharge should be removed between pulses and replaced by fresh gas. If this condition is not fulfilled, collisional de-activation of the vibrationally excited HF molecules and absorption of the radiation by ground-state HF molecules degrade the energy output of the laser.

The vibrational relaxation time of room-temperature HF is extremely short and has been measured²² as $\tau = 14 \text{ ns} - \text{atm.}$ As a consequence, the presence of only 1 to 2 torr of HF in the laser cavity completely quenches all laser action¹⁵.

In addition to self-quenching processes, vibrationally excited HF may be de-activated by V-V and V-R exchange collisions between HF and H_2 or hydrocarbon molecules. The more complex molecules, containing many hydrogen bonds, appear to be more effective in this respect, so that the optimum percentage of hydrocarbon in the gas mixture is lower than for hydrogen.

The effects of de-activation of HF by hydrogen compounds is clearly seen in Fig. 1, which shows the optical pulse energy as a function of propane concentration for an early HF/DF laser prototype. The production efficiency of F atoms in the glow discharge, the chemical formation rate of HF molecules and the quenching rates are all pressure dependent. Optimum operating pressures for an SF_6 - hydrocarbon mixture are between 40 and 100 torr (Fig. 2). Best discharge voltages range from 10 to 25 kV/cm, respectively.

With the addition of helium, the operating pressure of the laser may be increased up to atmospheric pressure¹⁰. The pulse energy, however, is decreased somewhat at higher pressures (Fig. 3).

Temporal gain measurements made by Marcus and Carbone¹⁵ in a typical pulsed HF laser at approximately 30 torr show the small-signal gain reaching a maximum at 0.6 μs after pulse initiation and then decaying rapidly due to collisional de-excitation to half its peak value within 1.5 microsecond. As a consequence, the optical pulse usually lasts less than 1 μs (except at very low gas pressures, below 10 torr)^{9, 20} and occurs within 0.5 μs of the leading edge of the current pulse. Accordingly, a current pulse which lasts longer than approximately 0.5 μs adds very little energy to the laser pulse. Maximum optical laser energy is, therefore, obtained with a short discharge pulse (small storage capacitor) of high energy content (high voltage). This behavior is confirmed in Fig. 4, which shows the output power and efficiency as a function of capacitor size for a prototype laser.

The early occurrence and short duration of the optical pulse also explains why bright arcs, which generally develop at the end of the current pulse, have little effect on the optical power output if the current pulse is longer than about 0.7 microsecond. As a result, the optical pulse-to-pulse amplitude stability of a hydrogen fluoride TE-laser is generally better than for a carbon dioxide TEA laser.

The performance curves in Figs. 1 to 5 were obtained with an early Lumonics prototype, which had an extremely slow gas exchange rate in the discharge tube (one change in 30 seconds) due to small pump size (50 l/min), restrictive pump lines and large discharge tube volume (15 cm diameter and 60 cm long). For convenience, the measurements were taken at a pulse frequency of 1 Hz, at which rate the HF accumulation in the optical cavity was already quite significant. As a consequence, the output energy per pulse and the electric efficiency were reduced to one third or less of their values at very low pulse repetition rates. In the gas flow range available, the optical output power varied linearly with volumetric gas exchange rate (Fig.5).

With more recent HF laser models, designed for more efficient gas exchange, optical pulses up to 500 mJ were obtained from a 50 cm long discharge (approximately 2 J/l) with efficiencies between 2.5 and 5% depending on pulse shape, electrode shape and applied voltage. Optical pulse energy was generally observed to increase linearly with increasing voltage up to approximately 15 to 20 kV per cm of discharge gap. At higher voltages, the pulse energy increased at a less than linear rate. Highest efficiencies are, therefore, obtained at lower voltages (<10 kV/cm).

Typical optical pulse shapes of an untuned HF laser are reproduced in Fig. 6. With SF_6 and H_2 the pulse width at the half-intensity points is 500 ns; with propane and other hydrocarbons it appears to be somewhat wider with a more slowly decaying trailing edge.

In general, only P-branch ($\Delta J = +1$) lines in the $v = 1 \rightarrow 0$, $v = 2 \rightarrow 1$ and $v = 3 \rightarrow 2$ vibration-rotation bands are observed in the output of a discharge-initiated HF/DF laser using SF_6 as the fluorine source. Even though most of these spectral lines are emitted superradiantly, it is possible to enhance any one of these by tuning the laser cavity with a diffraction grating. Spectral lines and wavelengths most often observed^{13, 18, 20} for HF are:

$P_1(3) - P_1(9)$	2.608 - 2.823 μ
$P_2(2) - P_2(9)$	2.696 - 2.954 μ
$P_3(3) - P_3(7)$	2.854 - 3.005 μ

For DF the transitions most readily observed are:

$P_1(5) - P_1(11)$	3.581 - 3.789 μ
$P_2(3) - P_2(12)$	3.636 - 3.957 μ
$P_3(3) - P_3(12)$	3.756 - 4.090 μ

In lasers having insufficient gas flow, some or all of the P_1 lines may be absent, since these are readily absorbed by ground-state HF molecules. In addition, collisional quenching may also prevent some of the rotational transitions in the P_1 , P_2 or P_3 bands from lasing.

IV SPECTRAL TUNING EXPERIMENTS

The requirements of high output energies, excellent tunability, single-mode operation and compact laser design cannot be met simultaneously with a superradiant laser. High pulse energies require a large discharge volume; good spectral resolution and single-mode operation can only be achieved with a long and narrow optical cavity. For low optical gain and good tunability, on the other hand, a short active laser length (a few cm) should be used. Reduction of the laser gain by other than geometrical means was, therefore, highly desirable for the success of this program.

It was evident from the start of the program that fulfillment of all performance specifications could only be achieved by one of two approaches.

Approach 1: Reduction of the small-signal gain per unit length of the laser to a point where dominant lines are no longer superradiant.

Approach 2: Removal of the unwanted superradiant spectral lines by means of a tunable filter.

There is no doubt that the first approach represents the more elegant solution of the two. Consequently, the primary research effort was channeled in this direction.

The least attractive way of reducing the gain of the active medium would be to operate the laser under conditions for which the collisional deactivation and optical absorption losses are increased.

This could be done by increasing the partial pressures of the fuel gases, by reducing the gas flow, by increasing the H/F-ratio of the fuel or by priming the reaction with a long electrical pulse. With all these methods, a significant amount of HF would accumulate during the pulse or from pulse to pulse. The result would be a severe loss in the optical pulse energy and a reduction in the number of spectral lines which could be tuned in.

Decreasing the H/F-ratio (hydrogen-starved operation) or decreasing the total pressure would also result in lower pulse energies. In addition, the optical pulse would be lengthened²⁰, and the peak power decreased to an unacceptably low level.

High efficiencies, but low optical pulse energies, may be attained with low electrical power input (small storage capacitor). This approach was taken by Ultee⁵, who achieved excellent spectral tunability, but obtained very low optical pulse energies (approximately $10 \mu J$ per pulse per line).

The most direct way of reducing the laser gain is to decrease the stimulated emission cross-section. This may be accomplished by operating the laser at higher gas pressures, where the collision-broadening of the vibrational energy states significantly exceeds the Doppler broadening. Because the optimum H/F-ratio and partial pressures of the fuel gases are restricted to low values by the chemical reaction rates and de-activation rates, the pressure can only be increased by adding an inert gas. Helium is a logical choice here, since it is known to add stability to a glow discharge at high pressure.

Control over the frequency and the mode of the optical laser beam can also be increased by employing an output reflector of high reflectivity (i.e. low output coupling). This establishes oscillation at the desired wavelength and in a low-loss mode early during the excitation pulse, when the gain has not yet built up to its maximum value. For the same reason, an unstable output reflector gives better spectral and mode control than an equivalent stable reflector (same output coupling), because the very high reflectivity (close to 100%) of the unstable reflector near the axis of the laser starts controlled laser oscillation earlier during the temporal gain build-up and, hence, at a lower gain per unit length. In addition, a properly designed unstable resonator favors single-mode oscillation, which in turn improves the spectral resolution of the line-tuned system. For all these reasons, the tuning experiments reported here were performed with an unstable mirror configuration (see Sec. Vc).

The electrical driving circuit and discharge electrodes of the experimental laser are shown schematically in Fig. 7. The discharge electrodes were 50 cm long and 3.5 cm apart. Approximately 11 J were stored in the 0.015 μ f capacitor and dumped across the discharge gap. A short pre-ionizing pulse between a row of metal pins and the cathode preceded the main pulse by approximately 0.5 μ s (a more detailed description of the discharge circuit is given in Sec. Va).

For the experimental data discussed in this section, the unstable output reflector was designed for 5% output coupling and an equivalent Fresnel number of one half. For intra-cavity tuning, a 2.6 μ Jarrell-Ash plane reflection grating with 295 lines/mm and a 4.0 μ Bausch and Lomb grating with 300 lines/mm were used with HF and DF, respectively.

To study the effects of gas pressure on the tunability and the mode control, measurements were taken at two widely different conditions. At both conditions, the glow discharge was relatively stable, with arcs occurring only infrequently. The gas compositions and pressures were:

1. Low-Pressure Mode at 45 Torr:

SF ₆	-	95%
H ₂ (D ₂)	-	5%
He	-	0

2. High-Pressure Mode at 550 to 600 Torr:

SF ₆	-	1.5%
H ₂ (D ₂)	-	0.5%
He	-	98%

HF spectra shown in Figs. 8 and 9 were recorded at the two pressure conditions by slowly scanning with the intra-cavity grating while pulsing the laser discharge at 2 pulses per second. The laser output was measured with a small thermopile (sensitive area 0.8 mm x 2 mm) placed near the inner edge of the annular laser beam. The signal from this detector was amplified and integrated and was then used to drive a millivolt chart-recorder operating at a slow chart speed. Scanning time for a complete spectrum was approximately 20 minutes. The apparent line widths were produced by "mode scanning" effects and by the long time constants of the integrator and recorder. The actual tuned power output of a specific line and of the untuned superradiant background were checked with a calibrated CRL thermopile power-meter for each recording.

Figure 8 illustrates the spectral line enhancement that can be obtained at an operating pressure of 45 torr by tuning the cavity. A maximum output of 125 mW was observed when the laser was tuned to the $P_1(7)$ line. A superradiant background of 20 mW was measured when the laser was detuned to a wavelength well outside of the vibrational HF-bands. At 550 torr (Fig. 9) maximum output was measured at 95 mW on the $P_2(5)$ line, and the background was found to be 8 milliwatt.

The spectral content of the untuned HF-laser output at low and high pressure is given in Figs. 10 and 11. These spectra were obtained by replacing the cavity grating with a flat reflector and analyzing the laser beam with an external monochromator (Czerny-Turner design made by McKee-Pedersen Instruments).

When deuterium was substituted for hydrogen, the tuned laser output (Fig. 12) at 45 torr showed a maximum average power of 70 mW on the $P_2(8)$ line and a low background of 8 milliwatt.

Close scrutiny of the data displayed in Figs. 8 to 11 permits the following conclusions to be drawn:

1. The ratio of maximum tuned line intensity to superradiant background is 6.25 at 45 torr and 11.9 at 550 torr. This indicates that the "tunability" of the superradiant HF-laser is enhanced at high pressures; i.e. the gain has been lowered by pressure-broadening of the energy states, as predicted.

2. The maximum tuned and untuned line intensities in each band occur at a lower rotational transition as the pressure is increased. This effect may be attributed to R-T energy exchanges between HF molecules and He atoms (rotational "cooling" of HF by helium).
3. Although the tuned output spectrum contains approximately the same spectral lines as the untuned laser beam, the relative line enhancement achieved by cavity tuning is more pronounced for lines of low rotational quantum number (e.g. lines 4 to 6 in the P_1 branch, lines 2 to 4 in the P_2 band and lines 2 and 3 in the P_3 branch).
4. The $P_1(5)$ line of HF and the $P_2(7)$ line of DF are inconsistently weak relative to their neighboring lines. The intensities of these lines can, however, be increased by filling the grating extension tube (1.5 m long) with helium. Evidently, these wavelengths are strongly absorbed by atmospheric H_2O and/or CO_2 .
5. For DF (Fig. 12), the ratio of maximum tuned line intensity to superradiance is 8.75 at 45 torr, somewhat higher than for HF. Hence, the optical gain with DF is naturally lower than with HF, making the DF laser more readily tunable.

The tuning experiments described above show that the optical gain can be lowered significantly without loss of pulse energy by going to higher gas pressures. As will be shown, however, the pulse shape reproducibility as well as the pulse energy stability of this laser are much poorer at high pressure than at low pressure.

Each vertical line in Fig. 13 represents the integrated optical pulse energy as obtained with a CRL power meter and at a gas pressure of 45 torr. Over the several hundred pulses recorded, the pulse energy variation is seen to be approximately $\pm 3\%$ at a pulse frequency of 1 Hz and approximately $\pm 8\%$ at 2 pulses per second. The deterioration of pulse-energy stability at higher pulse frequencies is caused by insufficient gas flow, which in turn results in the formation of streamers and arcs in the discharge.

The energy variation of the tuned laser output at 550 torr is greater than $\pm 30\%$ (Fig. 14), more or less independent of pulse frequency, and is not believed to be the result of streamer or arc formation. In fact, the observed pulse energy variations can be correlated with corresponding pulse shape variations, the cause of which has not been determined.

Optical pulse shapes were measured with a fast (rise time < 20 ns) room-temperature InSb photoconductive detector (Mullard RPY 78). All optical pulses measured have a half-width of approximately 500 ns (Figs. 15-17) except for the P_1 lines, which have a somewhat wider pulse (~ 700 ns). This suggests that the lasing levels in the first vibrational state are partially populated by cascading transitions from the higher vibrational levels. In all cases, lasing starts between 30 to 100 ns after initiation of the electrical pulse.

At 45 torr the optical pulses are smooth, single-peaked and have an excellent shape reproducibility. Note that each oscilloscope trace in Fig. 15 is made up of four consecutive pulses superimposed on each other. The same is not true at the high-pressure condition. Here, the pulse shapes exhibit a characteristic double-peak (Fig. 16), which has also been observed by Jacobson and Kimbell²⁰.

Furthermore, the pulse shape varies widely from pulse to pulse (Fig. 17) for this operating condition.

As discussed earlier, the use of an unstable output reflector improves the tunability of the laser. It also makes it possible to separate the superradiant background from the tuned line output, because the two components are emitted with widely differing beam divergences. The tuned output is single-mode and has a very low beam divergence (< 0.5 m rad), whereas the superradiant emission has a divergence at least ten times larger. In the far field, the superradiance is, therefore, quickly lost, and the central single-mode beam is close to 99% spectrally pure. The latter has been shown to be true by focusing the laser beam with a long-focal-length mirror and by passing the beam through a small aperture (consistent with a 1 m rad beam divergence) at the focal point. Approximately half the tuned near-field energy was measured on the far side of the aperture, yet no measurable superradiant background could be detected when the laser was detuned.

V DESCRIPTION OF LASER CONFIGURATION

Because of the unacceptably large variation in pulse energy and pulse shape at the high-pressure condition, the advantage of operating at a lower gain level could not be realized for the present system. Instead, the laser system was designed for use in the lower-pressure regime, and the spectral impurity background was removed with an external filter. The construction details and operating characteristics of the laser built for RADC are discussed in this section.

a) Electrodes and Discharge Circuit

Several features have been employed in the design of this laser to keep the formation of bright arcs in the discharge to a minimum. These are:

1. A smooth electrode profile with carefully rounded edges to assure a uniform electric field in the interelectrode gap,
2. A short current pulse (low circuit inductance) which stops the current flow before arc instabilities can develop,
3. A method of pre-ionization, that produces a uniform degree of ionization throughout the discharge volume before the main current pulse flows.

A schematic of the laser discharge circuit and the location of pertinent components are shown in Figs. 7 and 18. The internal structure of the laser discharge-tube consists of a perforated nickel cathode (K), a solid nickel anode (A) and a row of trigger pins^o serving as the pre-ionizer electrode. The main electrodes are 5 cm wide, 50 cm long and are separated by 3.5 cm.

The electric operating cycle consists of a slow charging phase, during which the storage capacitor ($0.015 \mu\text{f}$) is charged to 38 kV, and of a rapid discharge phase initiated by a high voltage trigger pulse, which fires the primary spark gap (SG1). A negative pulse, the energy of which is limited by the pre-ionizing capacitor, forms a fast glow discharge between the trigger pins and the cathode. This preliminary discharge generates electrons in the main gap by photoionization via ultraviolet light and soft X-rays and by electron penetration through the perforated cathode. Meanwhile (within 0.5 to $2 \mu\text{s}$), the auxiliary spark gap (SG2) has had time to break down and conduct the main current pulse to the cathode and through the gas in the inter-electrode region. The delay between pre-ionizing pulse and main pulse is controlled by the pressure in spark gap 2 and by the size of the cathode capacitor (500 pf). Owing to the rapid electron attachment to SF_6 and fluorine radicals (produced in the discharge), the pre-ionization is largely ineffective at 45 torr (95% SF_6). At 550 torr (1.5% SF_6), however, a definite improvement in discharge stability can be attributed to the pre-ionization technique.

b. Gas Flow and Controls

In order to prevent accumulation of HF in the discharge tube, the gas has to be pumped through the laser at a rapid rate. A 300 l/min mechanical pump is used in the present system to maintain the gas flow and the discharge-tube pressure at a constant level. Because of the relatively long 1 inch diameter pump-line, the actual measured pumping speed at the laser cavity is only 236 l/min (mostly SF_6). At this flow rate, the gas in the discharge tube is displaced every 0.7 seconds. Hence, the pulse energy remains constant with pulse repetition frequency (PRF) up to approximately 2 Hz.

At higher PRF, the pulse energy starts to decrease, even though the average power still increases up to 5 Hz. For lower PRF, the gas throughput may be reduced by throttling the flow to the pump and simultaneously decreasing the gas input at the flow meters (Fig. 19).

The individual gases are introduced through separate flow meters, brought together in a mixing manifold and passed into the laser tube. To protect the output reflector and the Brewster window (Fig. 20) from the corrosive reaction products, fresh gas is introduced at both ends of the laser tube and pumped out at the center. For similar reasons, the vacuum gauge and vacuum switch are connected to the input side, rather than the exhaust side of the gas flow system. Separate flow meters and supply lines are provided for the nitrogen supply to the spark gaps, which operate between 5 and 25 psi above atmosphere.

The vacuum switch has been added as a safety feature. When the pressure in the discharge tube rises above a preset value between 50 and 760 torr, the gas flow is turned off, and the HV supply is deactivated. This protects the laser tube from being pressurized above the operating range and from any uncontrolled effects of air leaks.

Solenoid valves at the gas input (Fig. 19) are used to automatically start or shut off the gas flow to the laser. This permits the gas flow to be electrically interlocked with other controls and sensing devices. It also makes it possible to leave the flow meters set at a predetermined flow rate when turning off the laser, facilitating subsequent rapid start-up.

c. Optical Design

The optical system (Figs. 20 and 21) of this laser includes the basic laser cavity, an external spectral filter (grating monochromator), a beam expander and two pulse energy monitors. The monochromator has been added to eliminate the superradiant background, which the high-gain laser emits in addition to the tuned wavelength. The beam expander reduces the beam divergence to a value which is suitable for atmospheric transmission measurements.

The laser cavity is formed by an unstable output reflector (U) and a reflective diffraction grating (G1 in Fig. 20). A sapphire Brewster window (B) separates the reactive gases from the grating.

UNSTABLE OUTPUT REFLECTOR:

The unstable CaF_2 output reflector has two convex surfaces and acts as a lens to collimate the output beam, which would otherwise diverge at an angle determined by the radius of curvature of the internal surface (45 m). A circular area, 8.2 mm in diameter, in the center of the inside surface of the lens has been gold-coated to reflect 75% of the incident wavefront back into the laser cavity. The remaining 25% of the wave are allowed to escape around the edge of the gold disc.

The curvatures and diameters of the front reflector surfaces are carefully matched to the cavity length and flat rear reflector (grating) to provide a high rejection ratio for all higher order transverse modes and to permit oscillation on the lowest order transverse mode only.

In the near field, the output beam consists of an annular ring defined by the diameter of the convex output mirror and the outer mode diameter. In the far field, the mode consists of a central circular beam of high intensity and a series of concentric diffraction rings. Approximately 1/4 to 1/3 of the near-field energy appears in the central spot in the far field. Proper choice of geometry insures that the principal maximum propagates with diffraction-limited divergence. For a more comprehensive treatment of unstable resonators, the reader is referred to the work by Siegman^{23,24}.

To understand the choice of cavity parameters, it is necessary to weigh carefully the following considerations:

1. For fundamental-mode operation of a TE laser, an unstable resonator makes use of a considerably larger volume of excited gas than a corresponding stable resonator. Hence the unstable cavity makes more efficient use of the available optical energy.
2. In view of the very high gain of a pulsed HF/DF laser, a relatively low optical output coupling <25% is necessary in order to have maximum control over the mode quality and spectral purity of the output beam.
3. The fraction of the near-field energy which appears in the central maximum of the far-field beam increases with increasing output coupling.
4. The near-field energy is a function of the active length, the gain per unit length, the percent output coupling and the mode of the laser output.

In the present design approximately equal importance has been attached to mode quality, reasonable control over spectral output and maximum energy in the far field.

WAVELENGTH SELECTOR:

Wavelength tuning is achieved with an adjustable intra-cavity diffraction grating, which forms the rear reflector of the optical resonator. A motor-driven precision micrometer (calibrated against wavelength) is used to greatly enhance any specific spectral line in the HF or DF spectrum (Figs. 8, 9, 12). The design of the grating mount and motor drive is illustrated in Figure 22.

The diffraction grating is a 300 line per mm "Bausch & Lomb" replica, blazed for a nominal wavelength of 4 microns. It has been found that this grating has a higher efficiency (80 to 90%) for both the HF and DF wavelengths than other available gratings blazed at lower wavelengths (2.6, 3.0, 3.5 microns).

SPECTRAL FILTER:

The external spectral filter (Figs. 20 and 21) is a modified Czerry-Turner Monochromator, designed to eliminate all but the spectral line for which the laser cavity is tuned. To increase the transmission efficiency, the entrance slit and the collimating mirror have been removed, and the laser beam is passed directly onto the diffraction grating. The grating is identical to that used in the laser cavity.

BEAM EXPANDER:

The basic beam expander (BE in Fig. 20) is a reflective confocal Cassegrain system with an f-ratio of 1.8 and an expansion ratio of 5. It is designed for a parallel incident beam of 2.0 cm diameter and provides a collimated output beam of 10 cm diameter. The degree of collimation can be adjusted by changing the distance between the two reflectors.

Because the near-field mode of the unstable resonator is ring-shaped, no beam energy is lost by the beam-obscuration due to the small convex reflector. The four spider vanes, however, cause some of the light energy to be diffracted out of the beam. A CaF_2 lens (L3) of 38 cm focal length has been added to the system (Fig. 20) to collimate the beam coming from the spectrometer slit before going into the beam expander.

BEAM DIVERGENCE:

The "far field" of a laser beam of diameter D may be defined as any distance from the source larger than the distance required for the peripheral rays of the laser beam to form a diffraction maximum at the center of the beam. This distance X_f may readily be shown to be

$$X_f = D^2/4\lambda \quad (4)$$

For a wavelength of 3μ and a beam diameter of 2 cm, this distance is 33 meter. For a 10 cm diameter beam, the far field recedes to a distance of approximately 800 meter.

It is, therefore, impractical to test the beam divergence by taking measurements in the far field directly. The far-field pattern may be brought arbitrarily close, however, by focusing the beam. This transforms the angular divergences into a displacement pattern. In the focal plane, the distance, Y , of an optical ray from the optical axis is related to its angular deviation θ by

$$Y = \theta f, \quad (5)$$

where f is the focal length of the lens or mirror. The energy distribution in the focal plane is a map of the angular energy variation in the far field, independent of whether the focusing element is placed into the near field or the far field of the beam.

Typical near and far-field beam patterns of the laser cavity itself are presented in Figure 23. The central maximum of the far-field beam has an elliptical shape, because of azimuthal non-uniformity in the near-field ring pattern. This uneven intensity distribution was produced by a corresponding non-uniform gain profile through the discharge gap.

The optical beam quality was improved after widening the discharge by reshaping the electrodes (with a 40% loss in optical pulse energy). Best far-field beam divergences were measured to be 0.35 m rad x 0.2 m rad for the central spot (Fig. 23).

A further reduction in beam divergence was accomplished by increasing the beam diameter to 10 cm with the 5:1 beam expander. Because of the large diameter, the near-field ring shape of the beam is maintained for several hundred meters (Fig. 24).

The far field was scanned with a 0.5 mm diameter aperture and a thermopile detector at the focus of a 25 m focal-length reflector. The half-width of the central peak was found to be 0.1 m rad x 0.2 m rad (Figs. 25 and 26). The non-symmetry of the "horizontal" profile is believed to be caused by the astigmatic and coma distortion due to the off-axis reflector in the monochromator. Because of the optical aberrations in the beam splitters, monochromator and beam expander, the reduction in beam divergence effected by widening the beam is only 1:2 instead of the theoretically possible value of 1:5.

VI PERFORMANCE SPECIFICATIONS OF DELIVERED SYSTEM

Input Power	- 115 VAC, 60 Hz
Laser Head Dimension	- 12"x20.8"x96"
Optical Platform	- 3.5"x30"x96" Structural Aluminum
Weight of Platform and Head	- 400 Lb.
Electrical Control Console and H.V. Power Supply	- 29"W x 24"D x 48"H
Gas Control Console and Vacuum Pump	- 29"W x 24"D x 48"H
Remote Tuning Control	- 10"W x 5"D x 3.5"H
Intra-Cavity Tuning	- 300 Lines/mm Diffraction Grating - manual and motor drive
External Spectral Filter	- Modified MP-1018-XM McKee-Pedersen Spectrometer with remote tuning and read-out (0.5 m F.L.)
Beam Expander	- 5:1 Cassegrain
Pulse Energy Monitors	- Two "Sensors" Thermopiles
High Voltage Input	- 0-50 KV (Variable)

Electrical PRF	- 0.5-20 Hz
Electrical Pulse Width	- 0.3 microsec (Half intensity points)
Gas Consumption	- SF_6 : up to 14 l/min (12 Lb/hr) H_2 (or D_2): 0.1 l/min N_2 (Spark Gaps): 0.8 l/min He (optional): up to 120 l/min
Lasing Mixture	- 95% SF_6 , 5% H_2 (or D_2) at 45 torr (Optional mixture: 98% He 1.5% SF_6 , 0.5% H_2 or D_2 at 550 torr)
Optical Wavelengths	- 18 Lines between 2.6 and 3.1 microns for HF - 24 Lines between 3.5 and 4.1 microns for DF
Optical Pulse Energies	- 40 mJ on dominant HF line at laser output, 24 mJ after spectral filter, 17 mJ after beam expander, 8 mJ in far-field beam. - 30 mJ on dominant DF line at laser output, 20 mJ after spectral filter, 13 mJ after beam expander, 6 mJ in far-field beam.

Far-Field Peak Power	- > 5 kW for at least 20 lines
Transmission Efficiencies	- Spectral Filter: 60% at 2.8 μ 67% at 3.8 μ - Beam Expander: 67%
Optical Pulse Width	- 500 nsec (half-intensity points)
Spectral Purity of Output Beam	- > 99%
Beam Diameter	- 10 cm
Modal Quality	- Fundamental transverse mode achieved with unstable resonator optics
Far-Field Beam Divergence of Central Maximum	- < 0.2 m radian
Probability of Pulse Occurrence	- > 99%
Pulse Energy Variations	- \pm 3% at 1 Hz \pm 8% at 2 Hz > \pm 10% at PRF > 3 Hz

VII CONCLUSIONS AND SUGGESTIONS FOR FUTURE DEVELOPMENT

It has been demonstrated that the gain of a pulsed chemical HF/DF laser can be lowered significantly without loss of optical energy when operated at high pressures. Improved tuning and mode control was obtained under those conditions. However, the pulse-to-pulse stability of energy and pulse shape was poor. In order to make full use of this operating regime, further studies are required to determine the cause for the pulse shape variations at high pressures. It may be possible to eliminate this problem by employing different pre-ionization techniques.

A special unstable output reflector was designed and tested. Additional control over the spectral output and the mode of the laser beam was gained by the use of this reflector.

To improve the uniformity of the annular output beam and, hence, the far-field divergence, future systems could be made of several discharge sections rotated with respect to each other. Furthermore, all auxiliary optics should be of extremely accurate surface figure to avoid beam distortion.

Finally, a line-tunable laser system with intra-cavity tuning and an external spectral filter and beam expander was built and delivered to the U.S. Air Force. The system performed satisfactorily and met most of the requirements set out at the beginning of the program.

VIII REFERENCES

1. J.C. Polanyi, J. Chem. Phys. 34 (1961) 347;
also Appl. Opt. Suppl. 2: Chem. Lasers 109 (1965).
2. J.V.V. Kasper and G.C. Pimentel, Phys. Rev. Letters 14
(1965) 352.
3. T.F. Deutsch, "Molecular Laser action in hydrogen
and deuterium halides", Appl. Phys. Letters 10
(1967) 234.
4. K.L. Kompa and G.C. Pimentel, "Hydrofluoric acid
chemical laser", J. Chem. Phys. 47 (1967) 857
5. C.J. Ultee, "Compact pulsed HF lasers", Rev. Scient.
Instr. 42 (1971) 1174, also IEEE J. Quant. Electron.
QE-6 (1970) 647.
6. M.C. Lin, "Chemical HF laser from $\text{NF}_3\text{-H}_2$ and $\text{NF}_3\text{-C}_2\text{H}_6$
systems", J. Phys. Chem. 75 (1971) 284.
7. R.J. Jensen and W.W. Rice, "Electric discharge initiated
 $\text{SF}_6\text{-H}_2$ and $\text{SF}_6\text{-HBr}$ chemical lasers", Chem. Phys.
Letters 7 (1970) 627.
8. T.V. Jacobson and G.H. Kimbell, "Transversely spark-
initiated chemical laser with high pulse energies",
J. Appl. Phys. 41 (1970) 5210.
9. T.V. Jacobson and G.H. Kimbell, "Transversely pulse-
initiated chemical lasers; Preliminary performance
of the HF system", Chem. Phys. Letters 8 (1971) 309.

10. T.V. Jacobson and G.H. Kimbell, "Transversely pulse-initiated chemical lasers: Atmospheric-pressure operation of an HF laser", J. Appl. Phys. 42 (1971) 3402.
11. W.H. Green and M.C. Lin, "Pulsed-discharge initiated chemical lasers: III. Complete population inversion in HF", J. Chem. Phys. 54 (1971) 3222.
12. O.R. Wood, E.G. Burkhardt, M.A. Pollack and T.J. Bridges, "High-pressure laser action in 13 gases with transverse excitation" Appl. Phys. Letters 18 (1971) 261.
13. O.R. Wood and T.Y. Chang, "Transverse-discharge hydrogen halide lasers". Appl. Phys. Letters 20 (1972) 77.
14. S. Marcus and R.J. Carbone, "Performance of a transversely excited pulsed HF laser, "IEEE J. Quant. Electron. QE-7 (1971) 493.
15. S. Marcus and R.J. Carbone, "Gain and relaxation studies in transversely excited HF lasers, "IEEE J. Quant. Electron. QE-8 (1972) 651.
16. T.F. Deutsch, "Parameter studies of pulsed HF lasers," IEEE J. Quant. Electron. QE-7 (1971) 174.
17. H. Pummer and K.L. Kompa, "Investigation of a 1 J pulsed discharge-initiated HF laser", Appl. Phys. Letters 20 (1972) 356.

18. Lumonics HF/DF laser performance sheets (1971).
19. R.G. Wenzel and G.P. Arnold, "A double-discharge initiated HF laser" IEEE J. Quant. Electron QE-8 (1972) 26.
20. T.V. Jacobson and G.H. Kimbell, "Parametric studies of pulsed HF lasers using transverse excitation", IEEE J. Quant. Electron QE-9 (1973) 173.
21. R.J. Jensen and W.W. Rice, "Thermally initiated HF Chemical laser", Chem. Phys. Letters 8 (1971) 214.
22. J.R. Airey and S.F. Fried, "Vibrational relaxation of hydrogen fluoride", Chem. Phys. Letters 8 (1971) 23.
23. A.E. Siegman, "Stabilizing output with unstable resonators" Laser Focus (May 1971) 42.
24. A.E. Siegman and H.Y. Miller, "Unstable optical resonator-loss calculations using the Prony method" Appl. Optics 9 (1970) 2729.

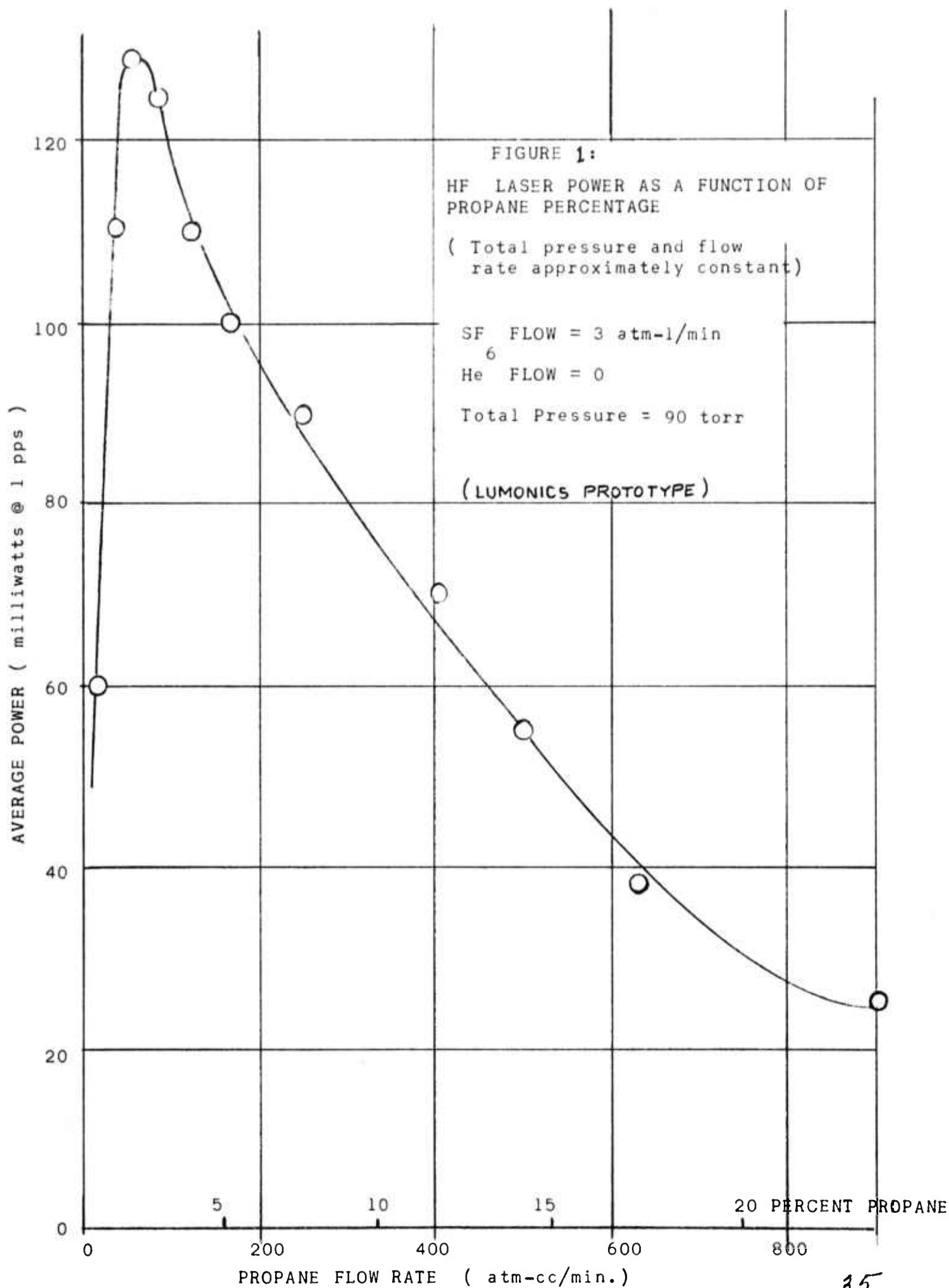
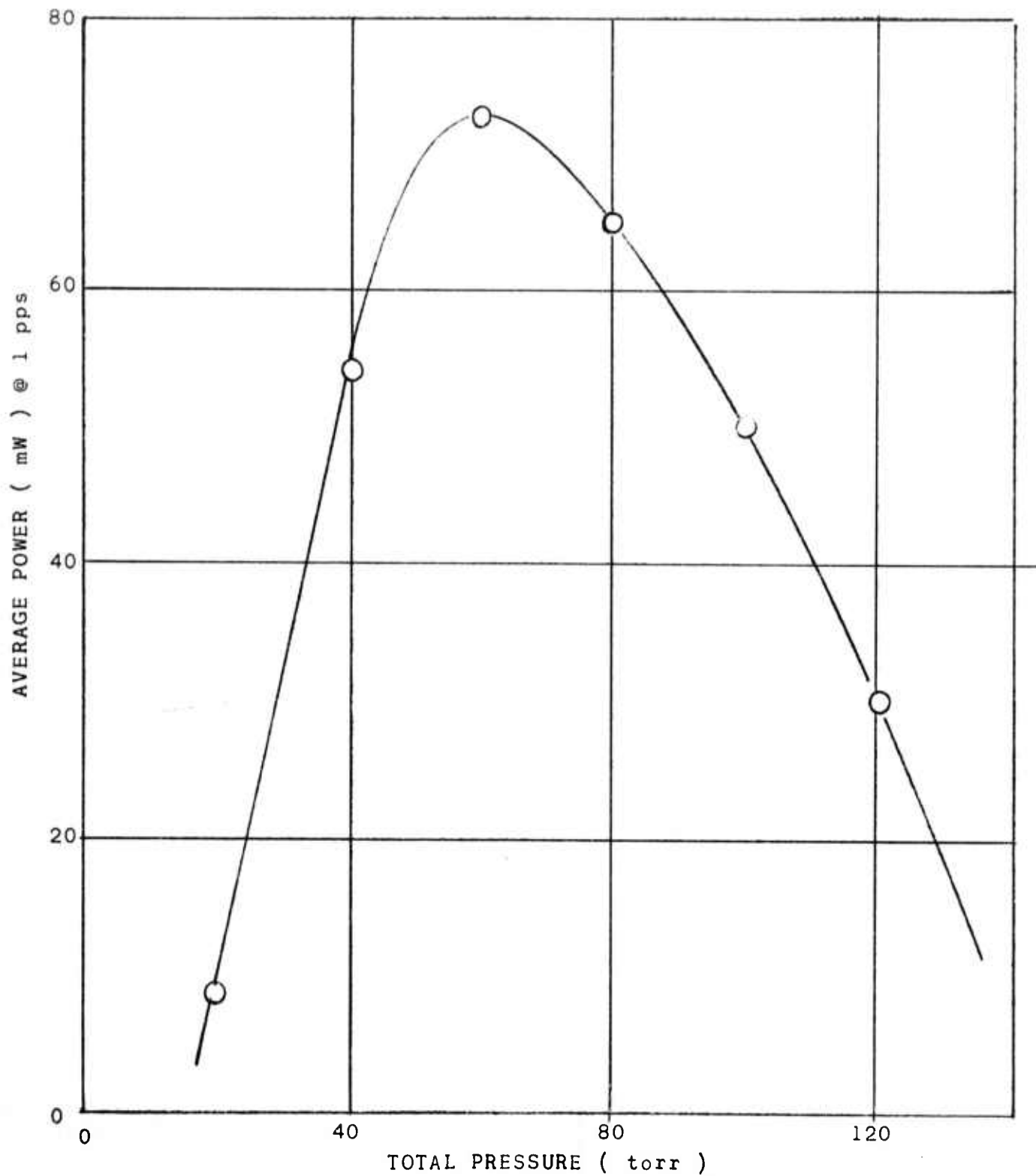
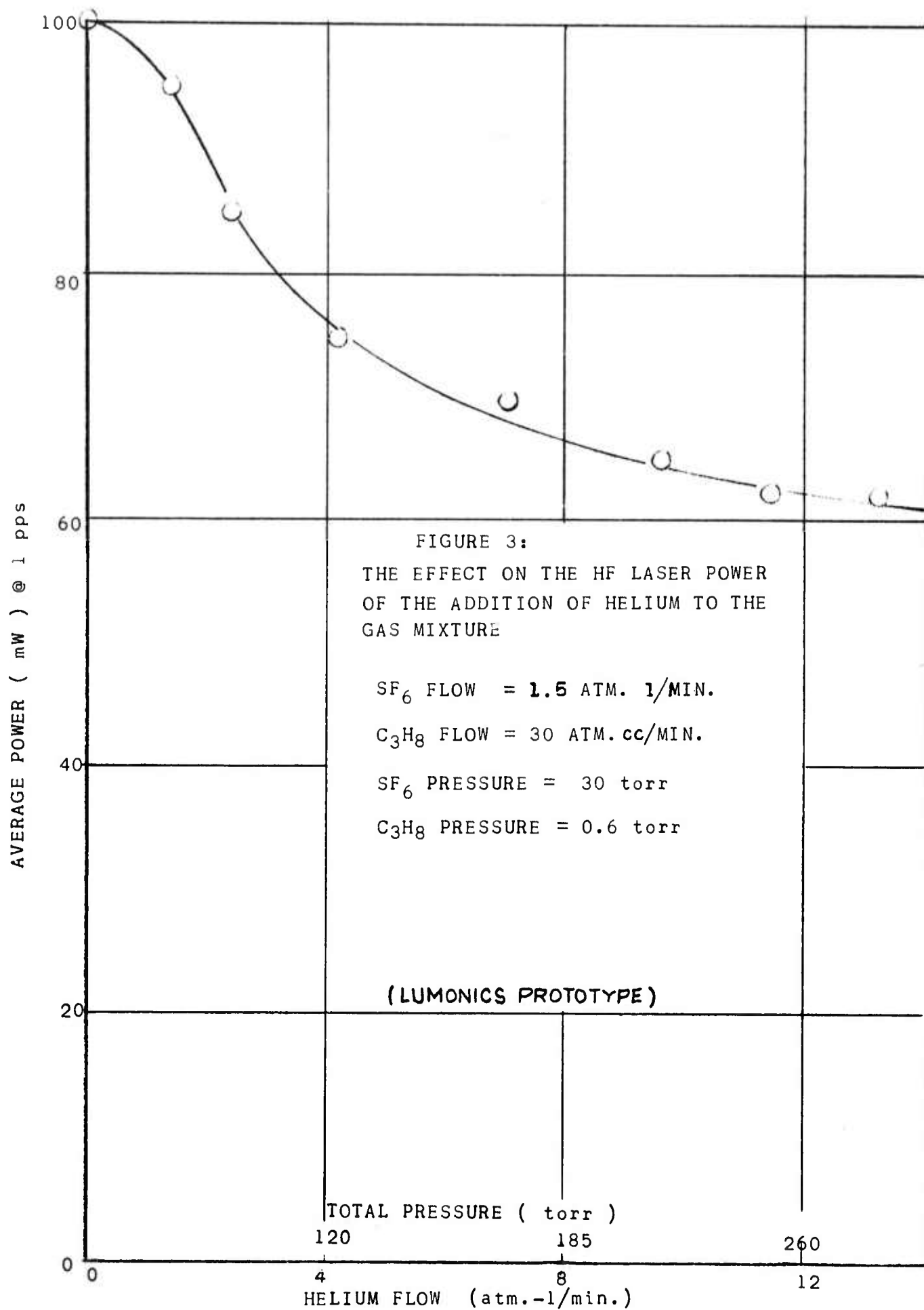


Figure 2:

HF LASER POWER AS A FUNCTION OF GAS PRESSURE AT CONSTANT FLOW
VELOCITY AND CONSTANT COMPOSITION (LUMONICS PROTOTYPE)

$\text{SF}_6 : \text{C}_3\text{H}_8 : \text{He} = 50 : 1 : 0$; Volumetric Flow Rate = 19.5 l/min.





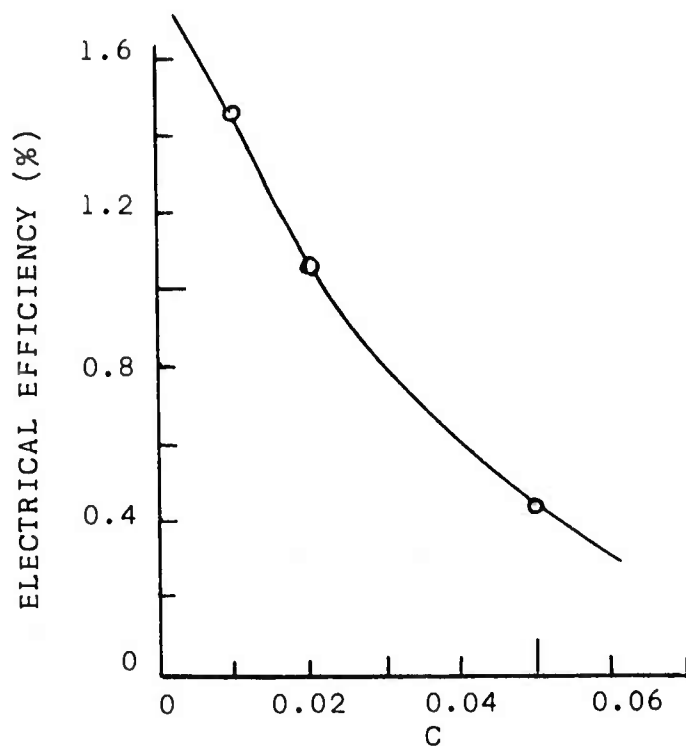
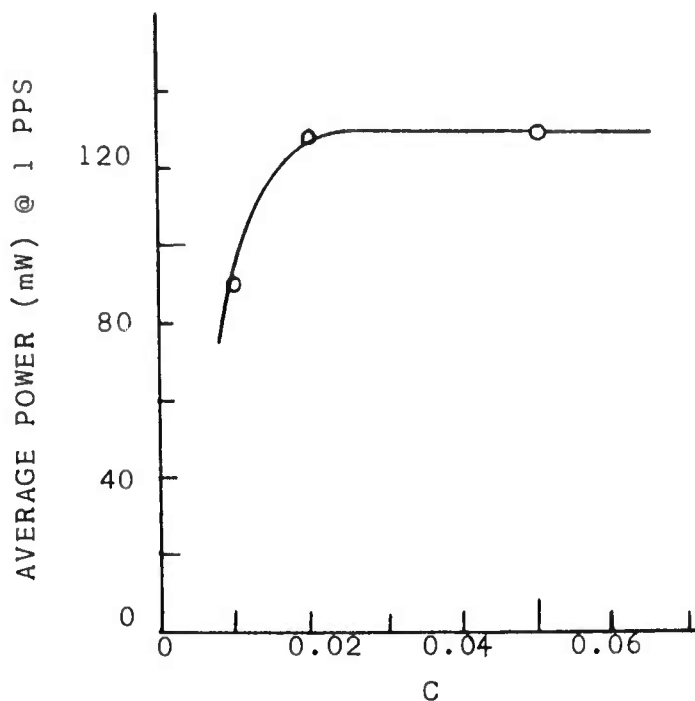
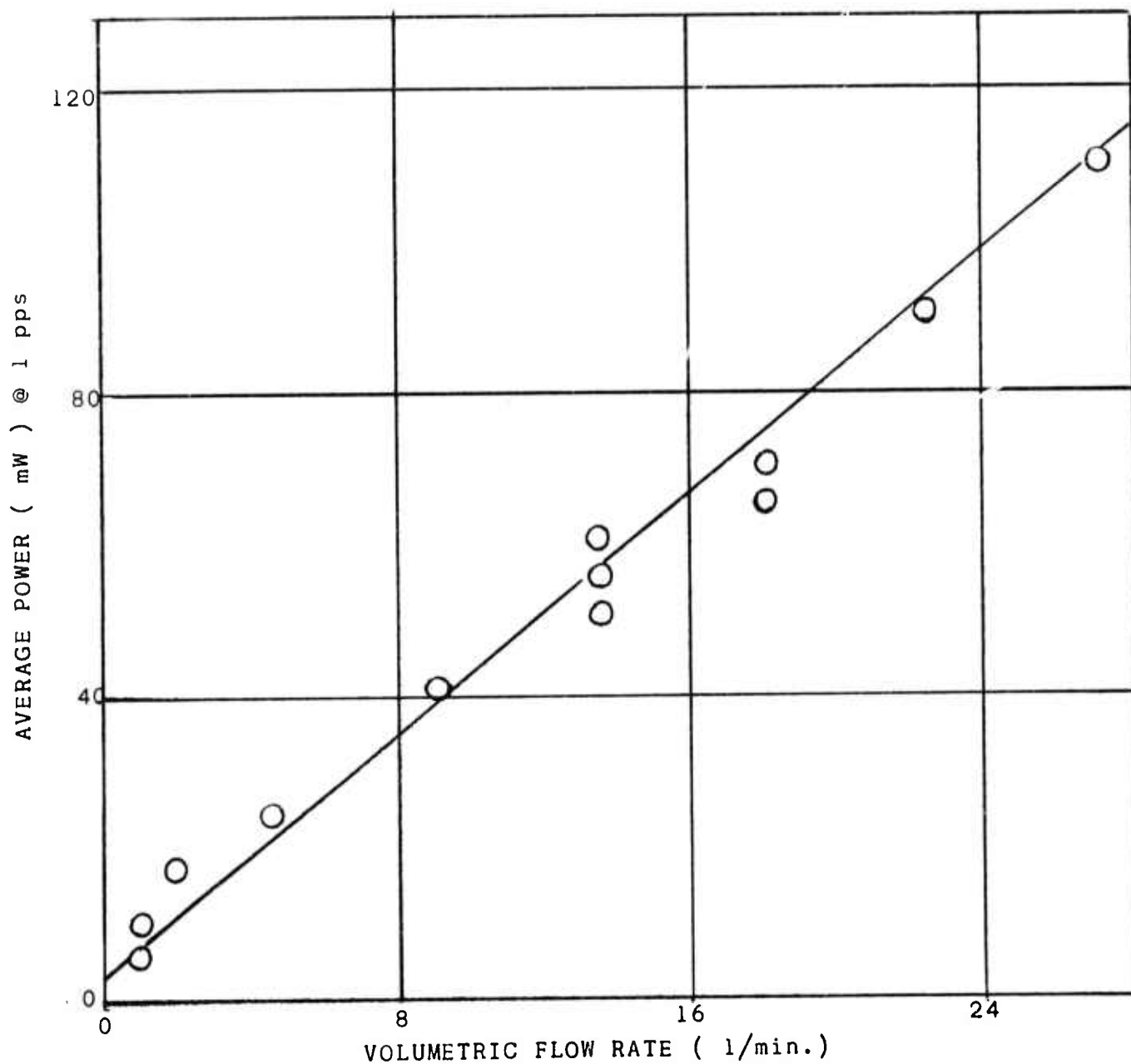


FIGURE 4: OUTPUT POWER AND EFFICIENCY AS FUNCTION OF CAPACITOR SIZE (PULSE WIDTH) AT 35 KV (LUMONICS PROTOTYPE)
 SF_6 FLOW = 3 atm - l/min
 C_3H_8 FLOW = 0.06 atm - l/min
 $P = 86$ TORR

FIGURE 5:

HF LASER POWER AS A FUNCTION OF FLOW VELOCITY AT CONSTANT
PRESSURE AND COMPOSITION (LUMONICS PROTOTYPE)

Total Pressure = 85 torr; SF_6 : C_3H_8 : He = 50 : 1 : 0



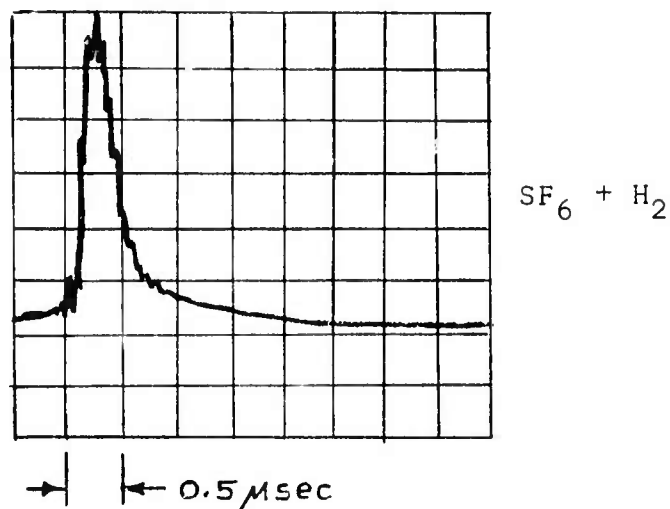
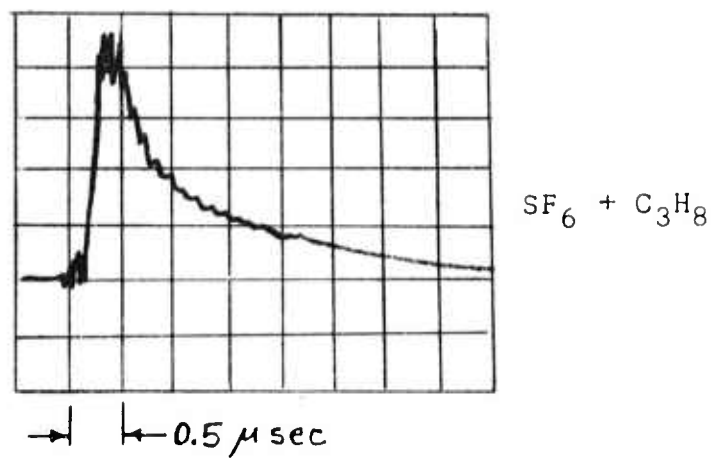


FIGURE 6: HF-LASER OPTICAL PULSE SHAPES OBTAINED WITH
PHOTON DRAG DETECTOR
(PRESSURE = 50 TORR)

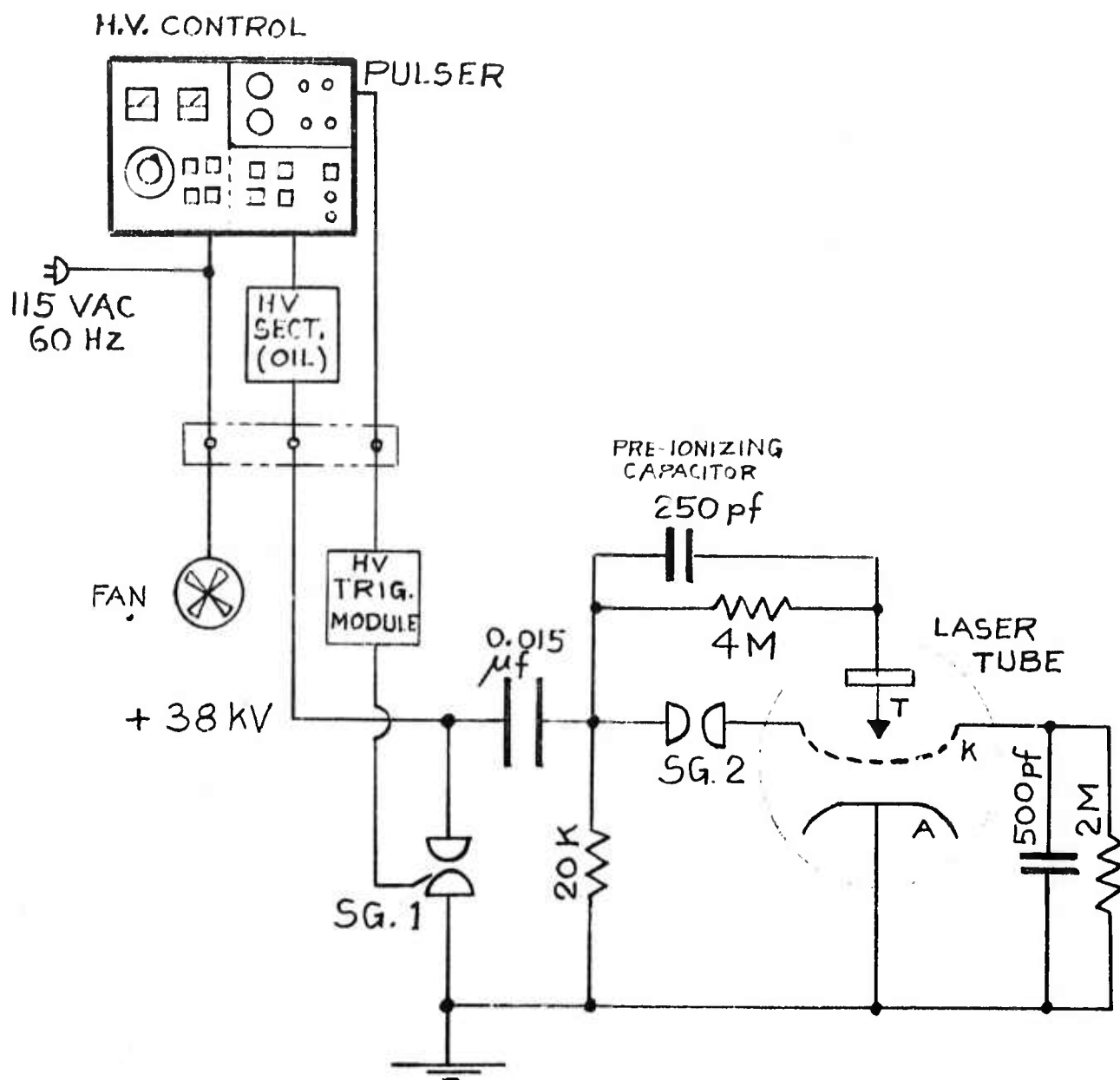


FIGURE 7:
LASER DISCHARGE CIRCUIT

47

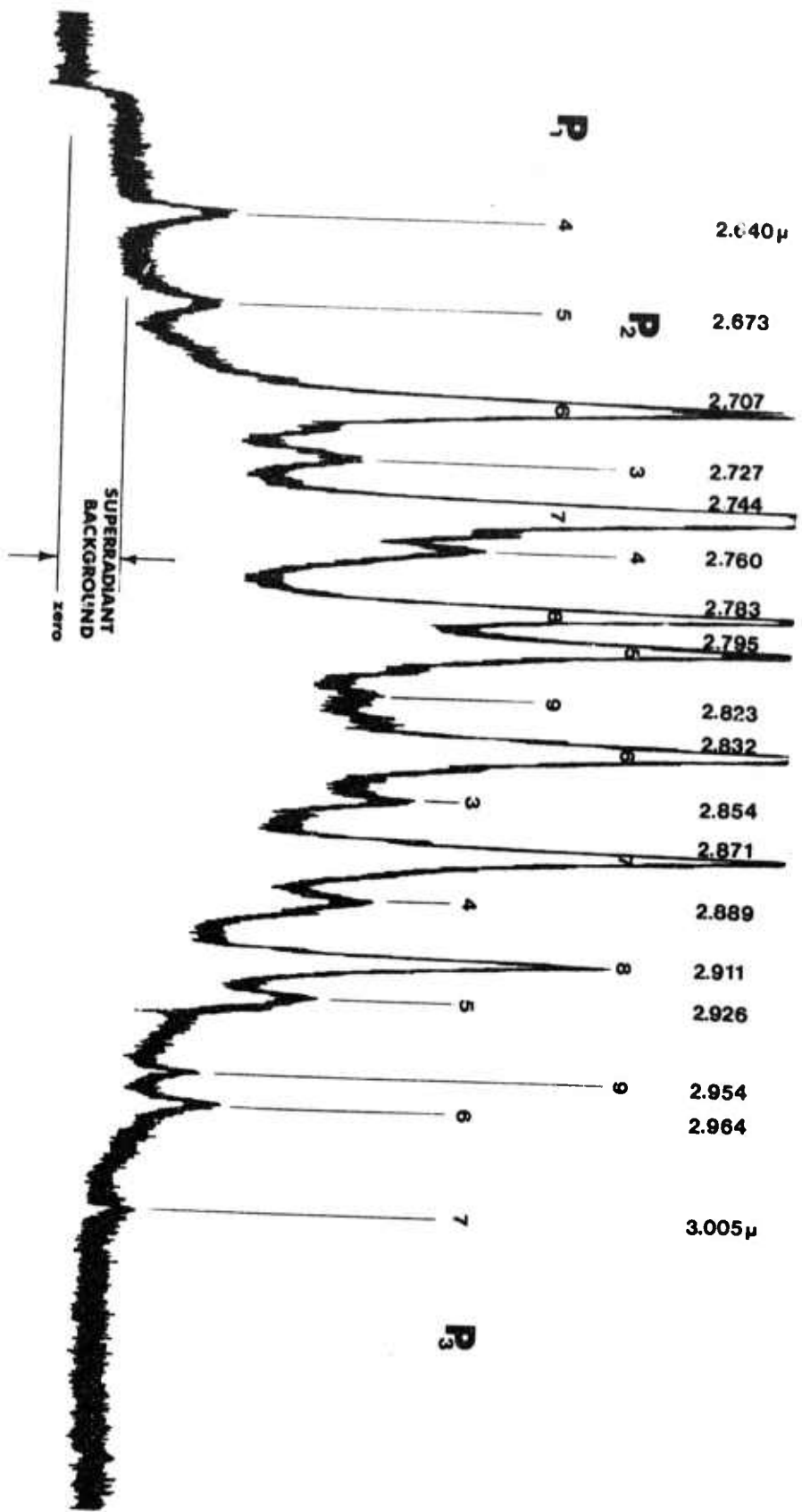


FIGURE 8: HF LASER OUTPUT SCANNED WITH INTIPA-CAVITY GRATING (P = 45 TORR)

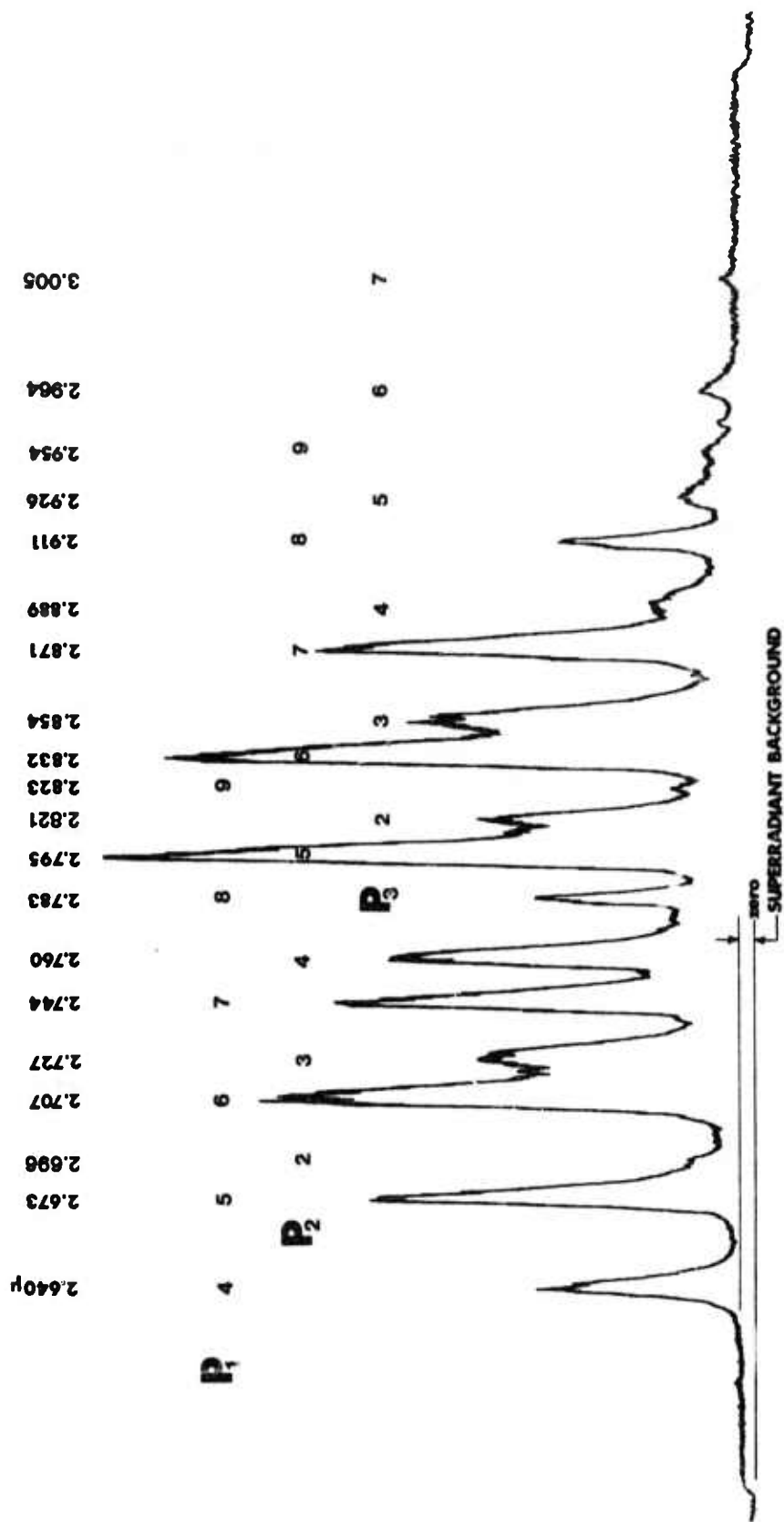


FIGURE 9: HF LASER OUTPUT SCANNED WITH INTRA-CAVITY GRATING (P = 550 TORR)

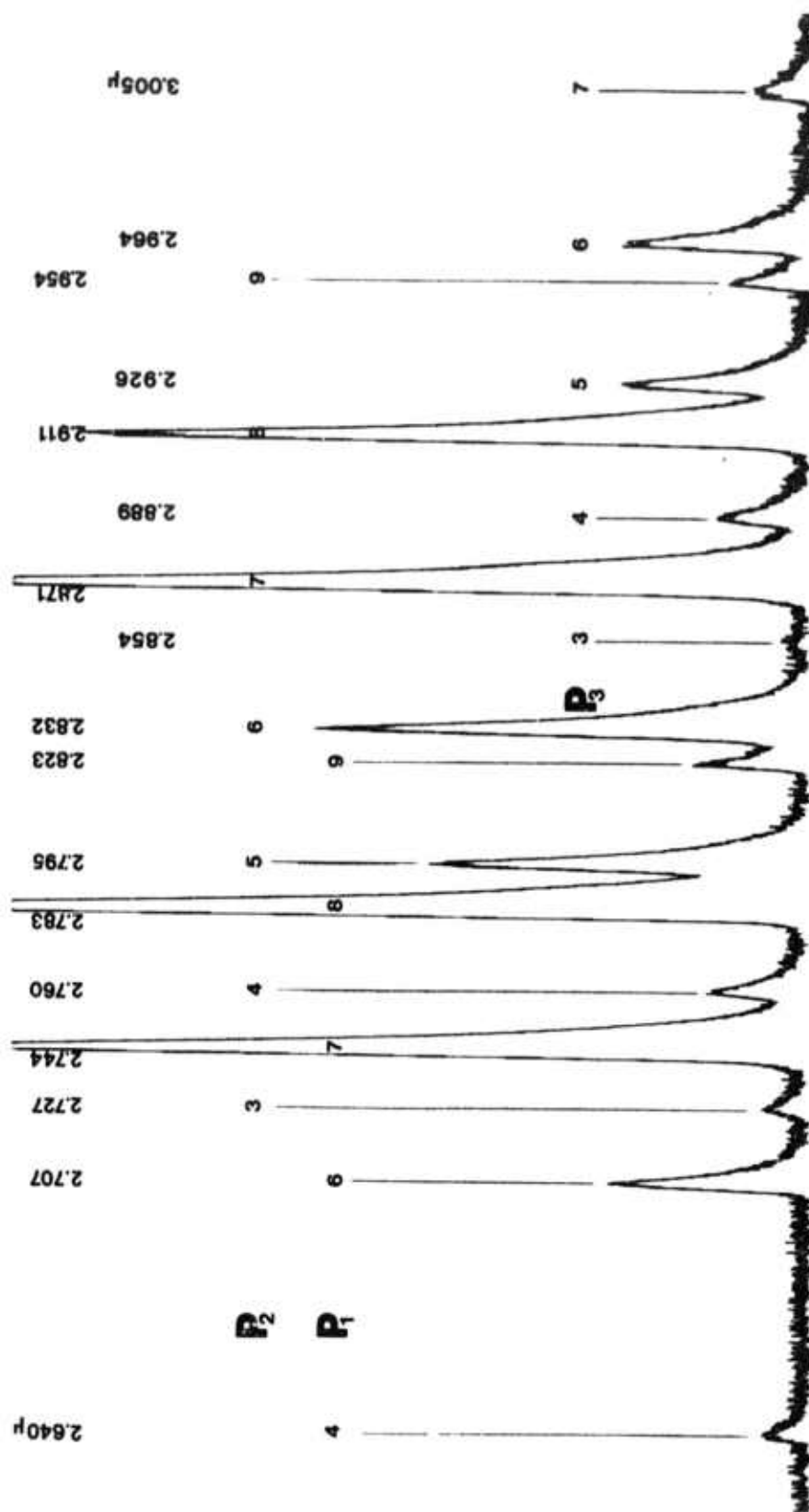


FIGURE 10: HF - SPECTRUM OF UNTUNED LASER EMISSION SCANNED WITH EXTERNAL SPECTROMETER
(P = 45 TORR)

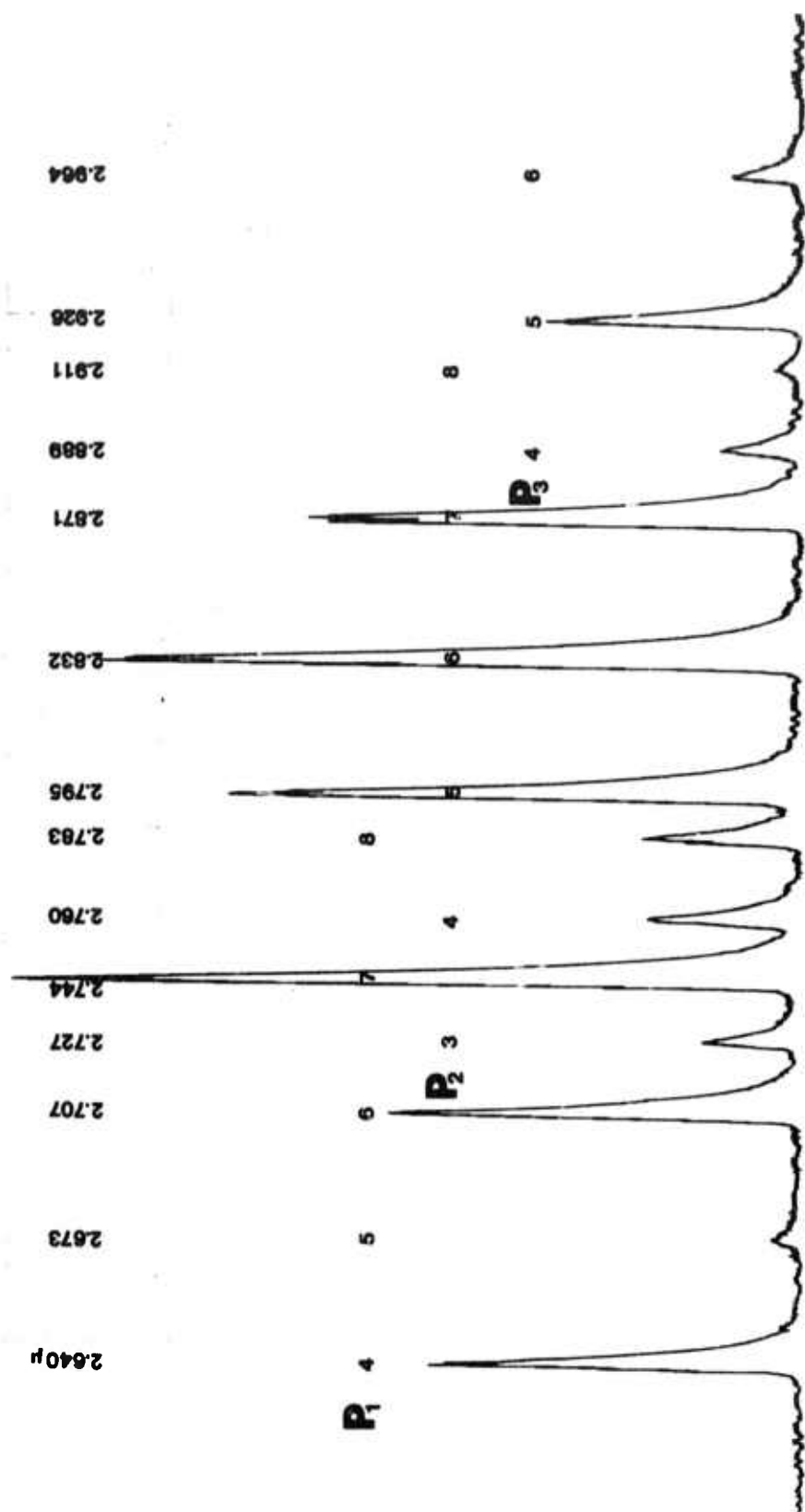


FIGURE 11: HF - SPECTRUM OF UNTUNED LASER EMISSION SCANNED WITH EXTERNAL SPECTROMETER
(P = 580 TORR)

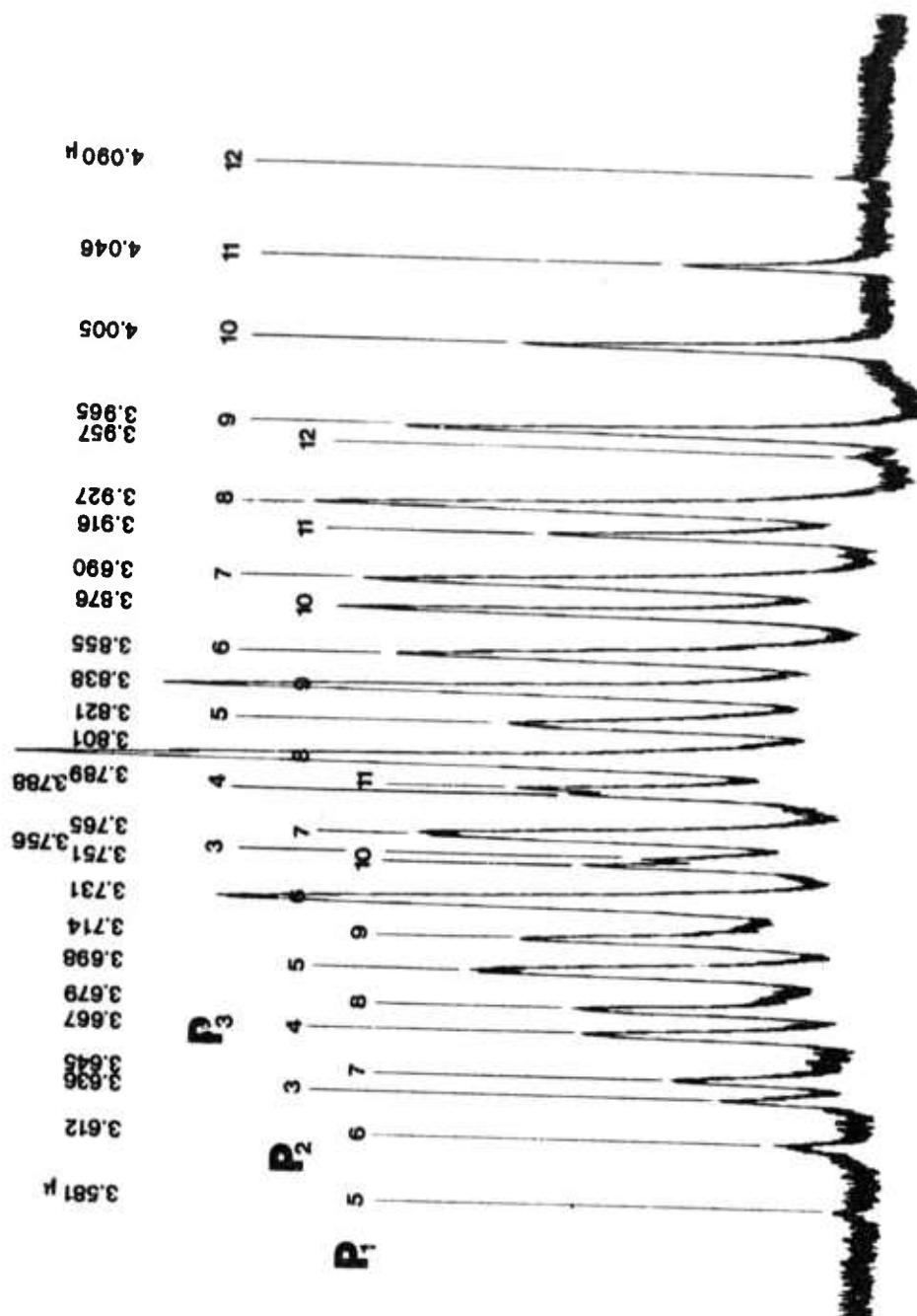
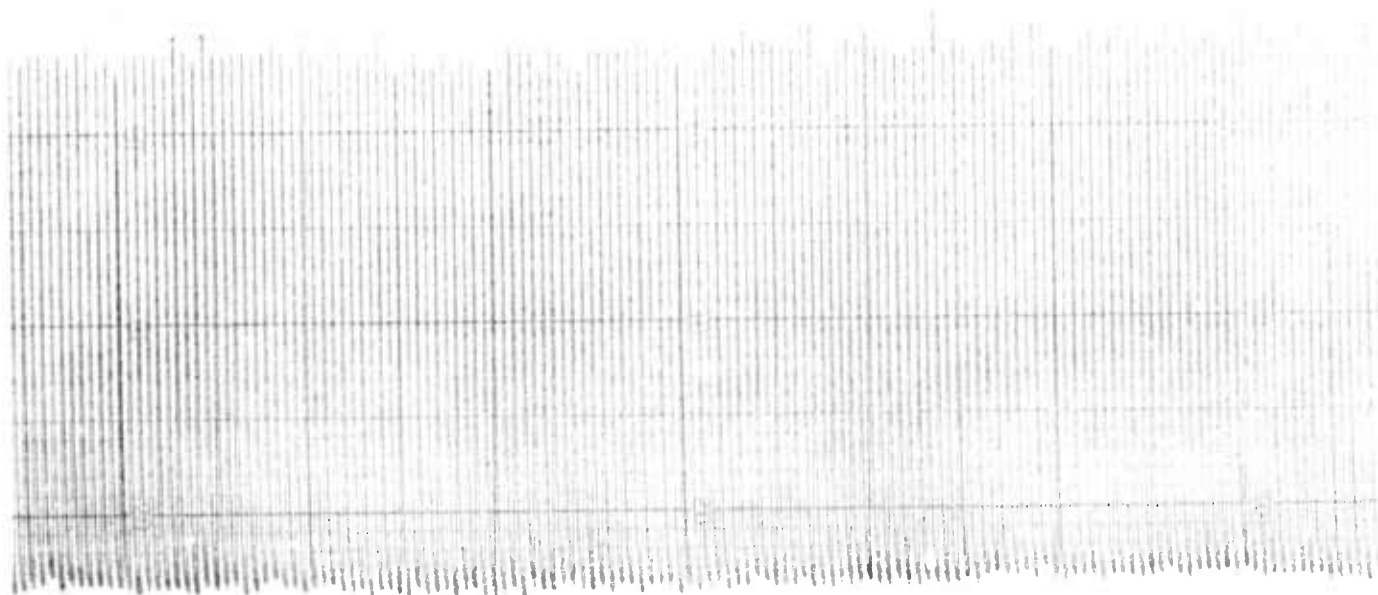
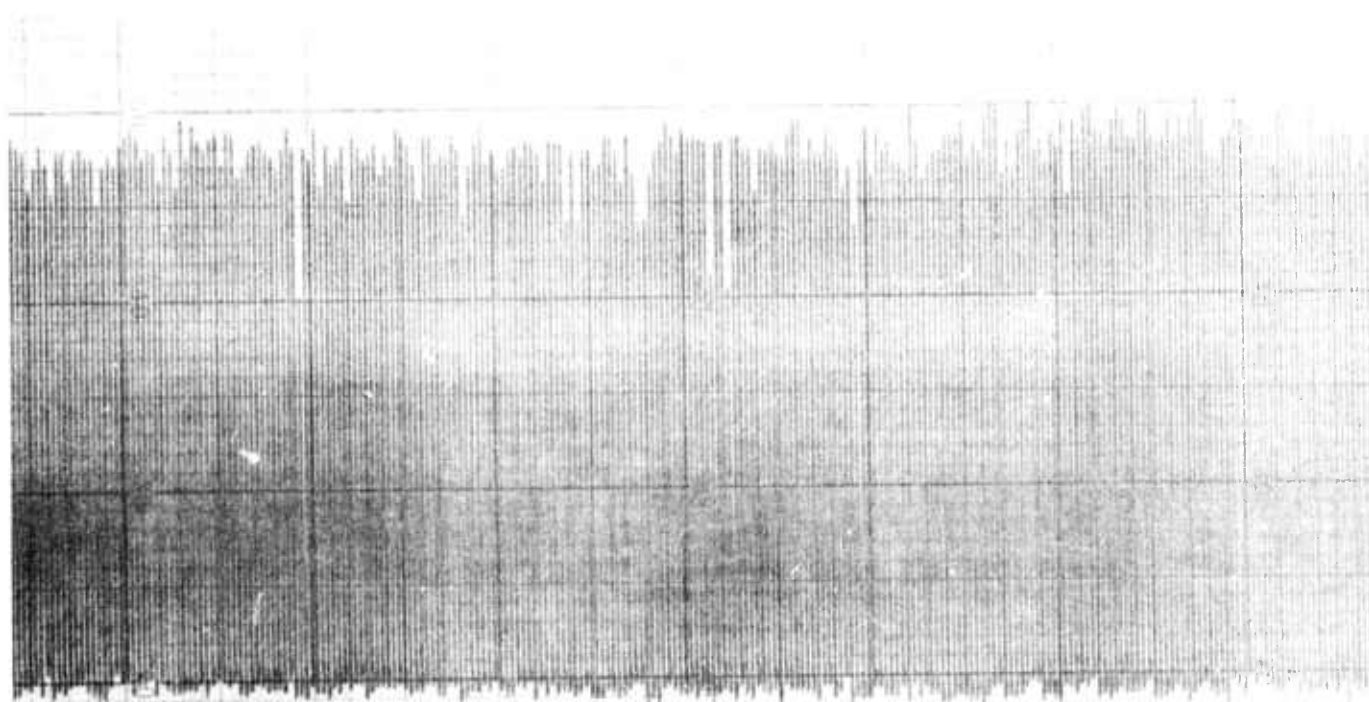


FIGURE 12: DF LASER OUTPUT SCANNED WITH INTRA-CAVITY GRATING (P = 45 TORR)

**Pulse Energy Variation of Laser Output Tuned to
HF - $P_1(7)$ Line (p = 45 torr)**



at 1 Hz



at 2 Hz

FIGURE 13

Energy Variation of Tuned Laser Output at 550 torr (with HF)

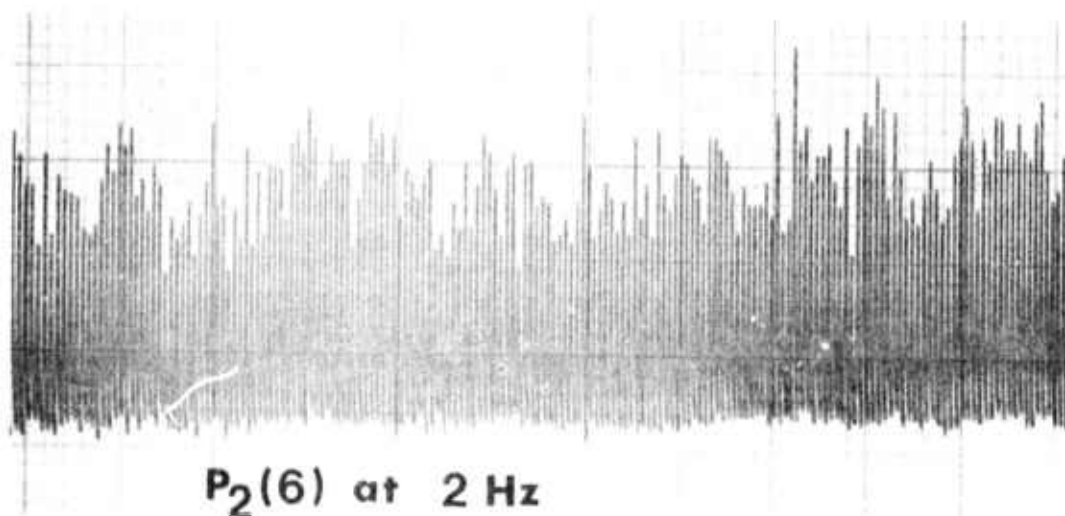
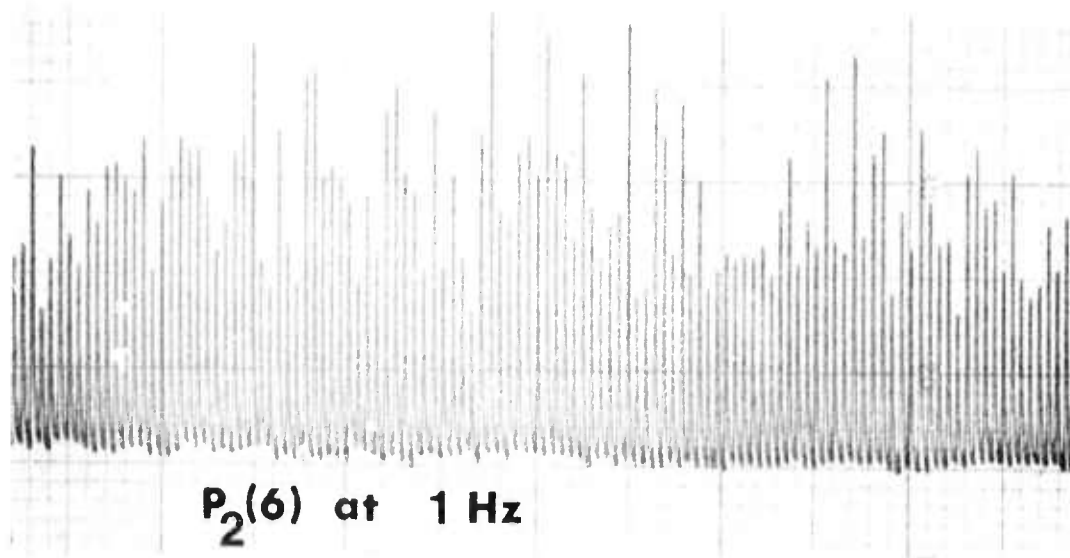
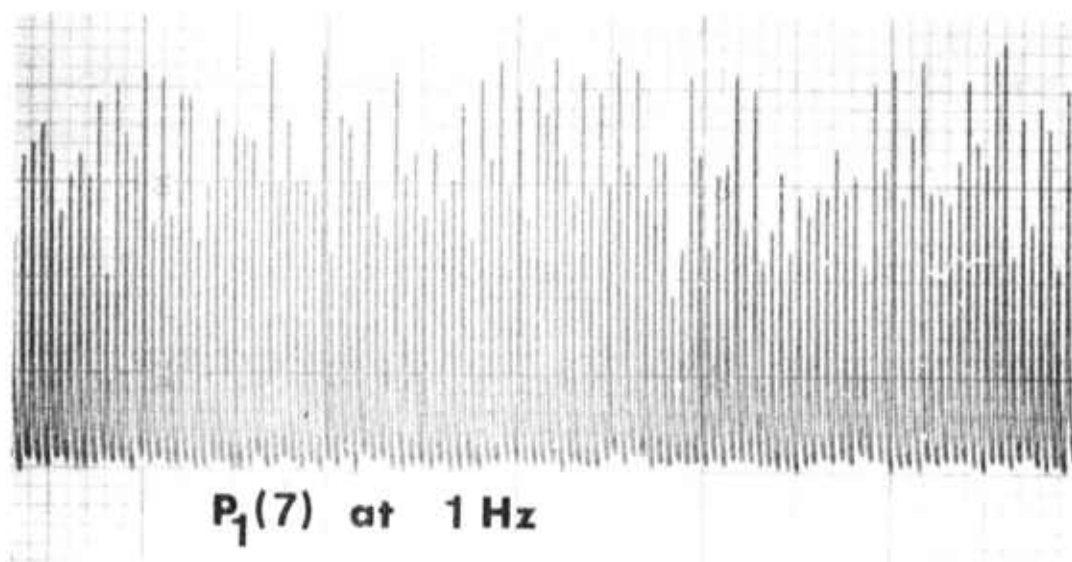
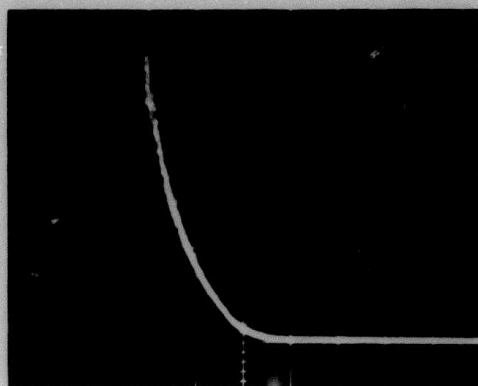


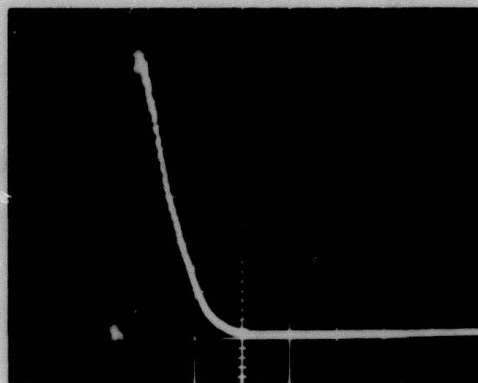
FIGURE 14



$P_1(7)$

500 ns per cm

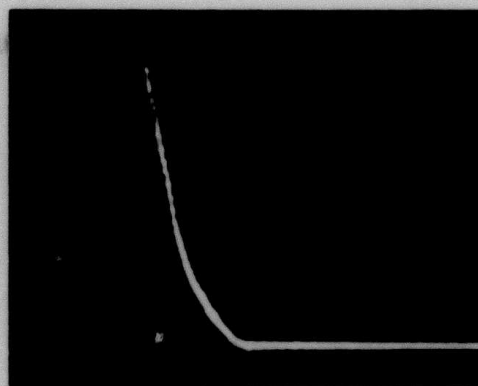
↑
Start of electrical discharge



$P_2(6)$

500 ns per cm

← 500 ns



$P_3(6)$

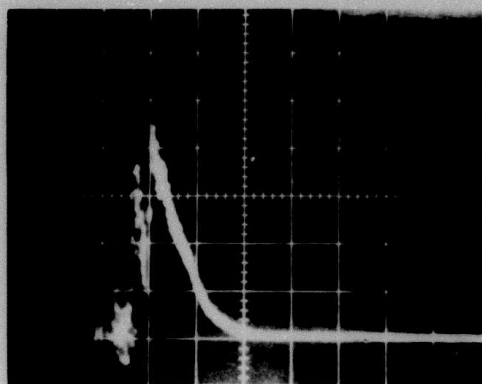
500 ns per cm

FIGURE 15:

OPTICAL PULSE SHAPES OF HF-LASER (4 pulses superimposed)

Pressure: 45 Torr, 6% H_2 , 94% SF_6

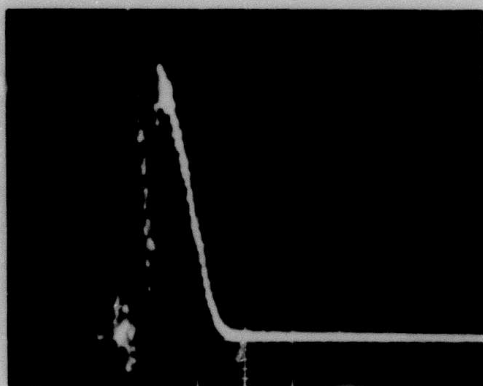
Detector: Mullard RPY 78 InSb Photoconductive Film



$P_1(7)$

500 ns per cm

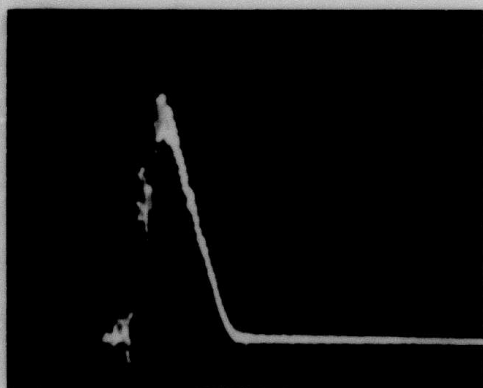
↑
Start of electrical discharge



$P_2(6)$

500 ns per cm

← 500 ns



$P_3(6)$

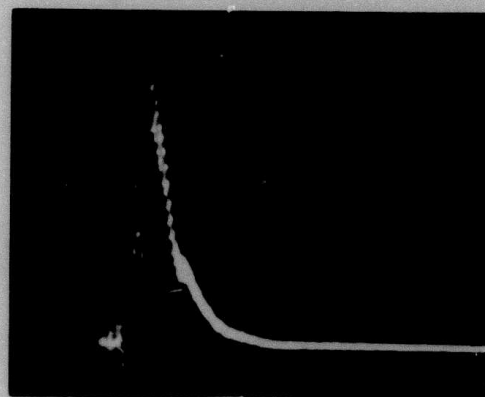
500 ns per cm

FIGURE 16:

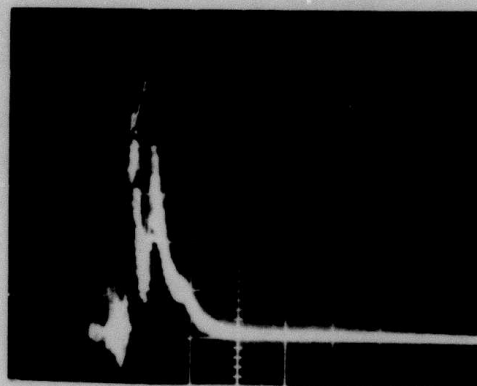
OPTICAL PULSE SHAPES OF HF-LASER (single pulse)

Pressure: 550 Torr, 98% He, 1.5% SF_6 , 0.5% H_2

Detector: Mullard RPY 78 InSb Photoconductive Film



↑ Start of electrical discharge



→ ← 500 ns

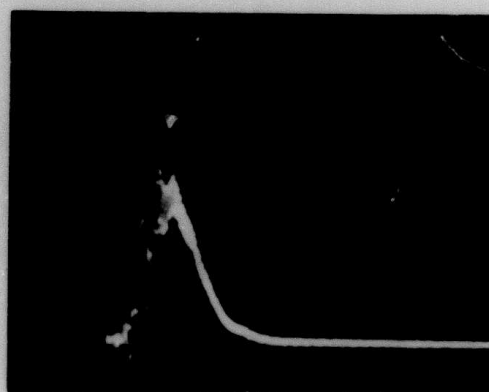


FIGURE 17:

PULSE-TO-PULSE VARIATION OF $P_1(7)$ LINE (HF) AT 550 TORR

98% He, 1.5% SF_6 , 0.5% H_2

Detector: Mullard R9Y 78 InSb Photoconductive Film

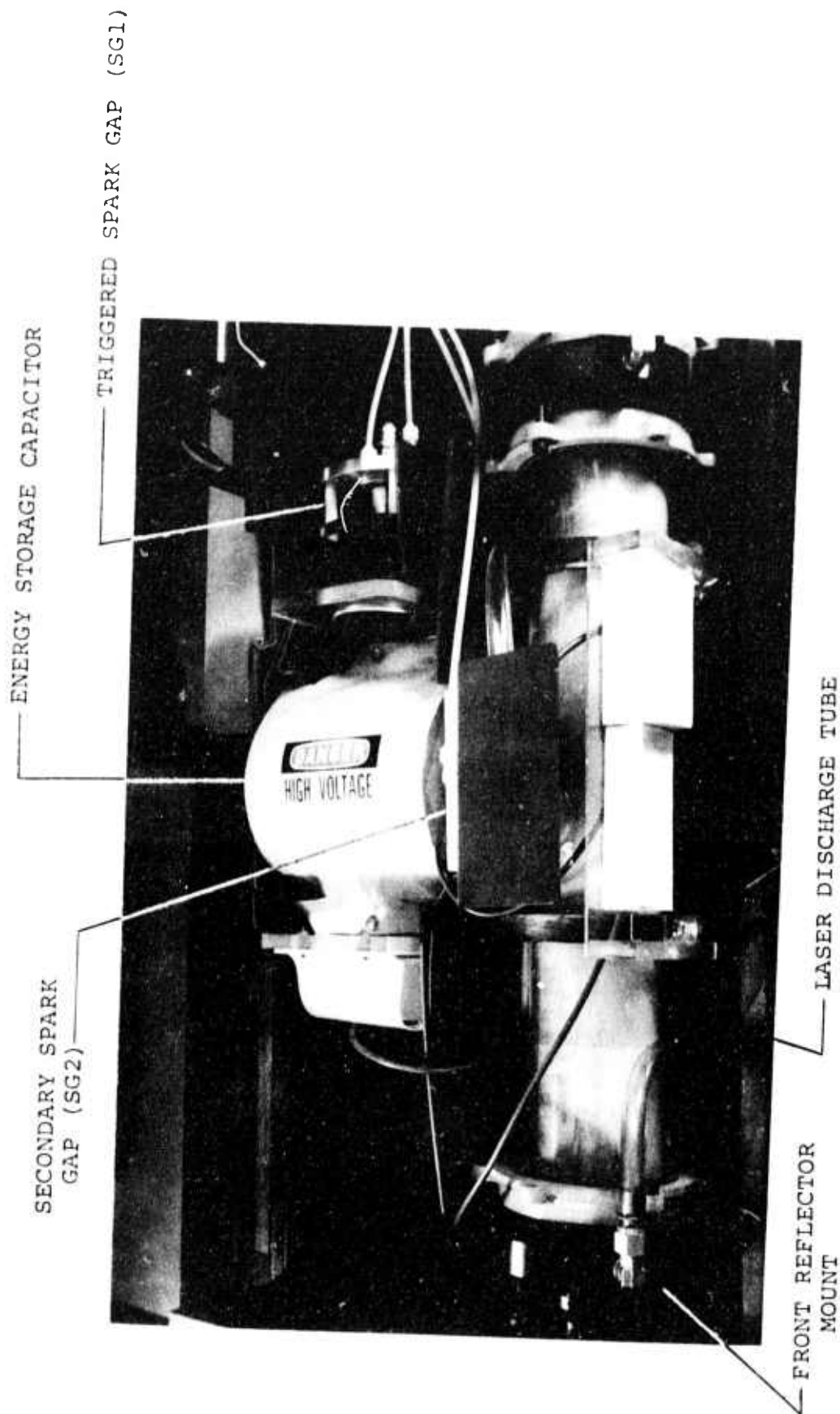
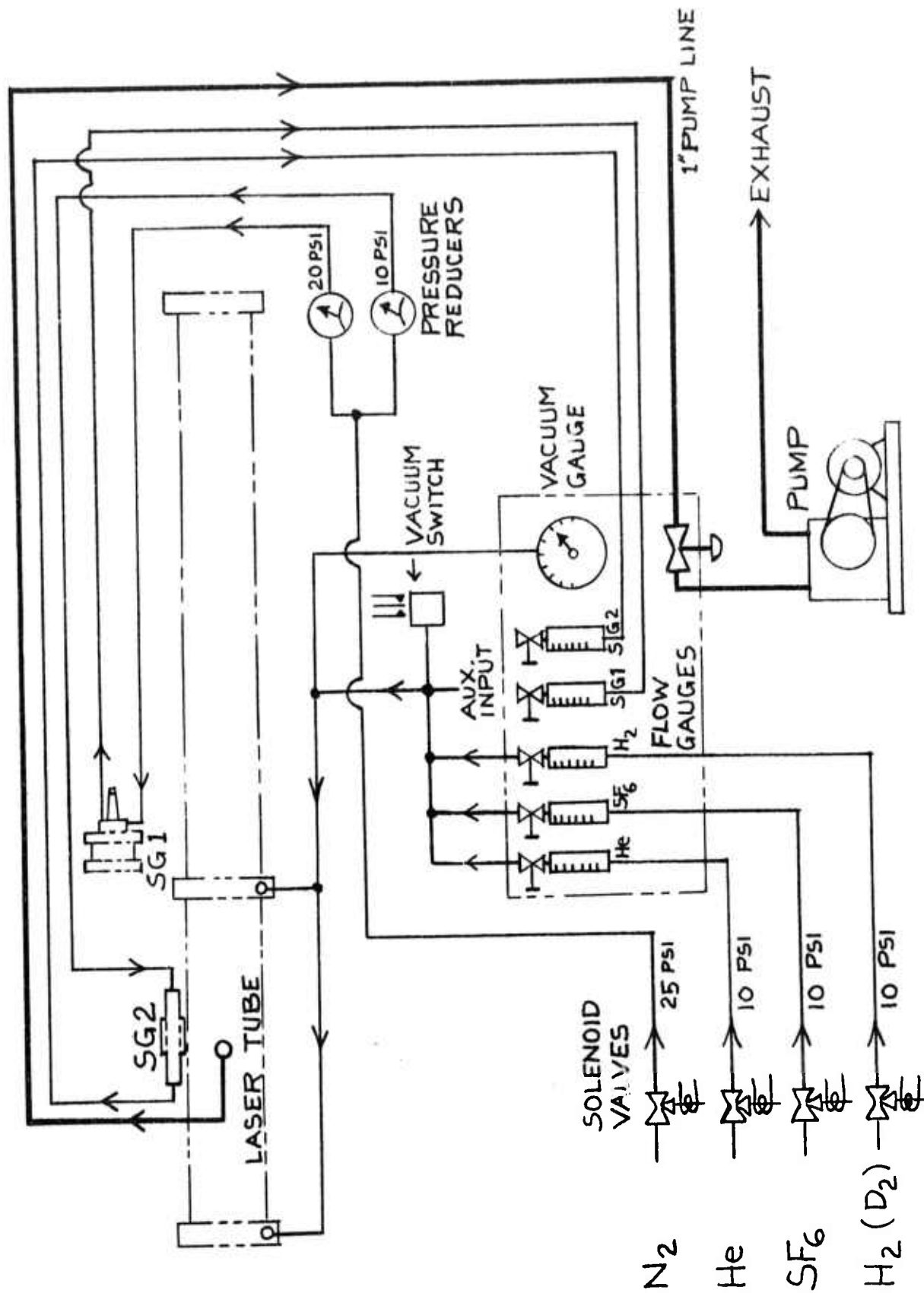


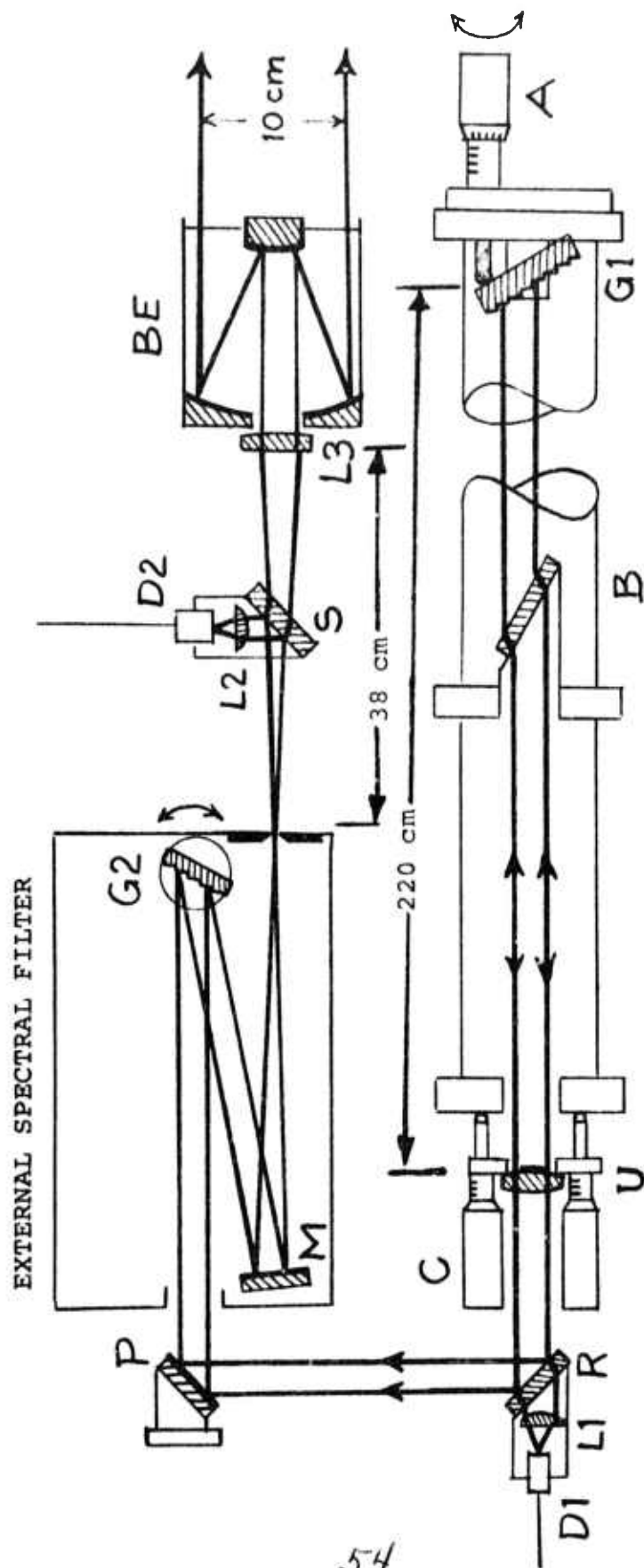
FIGURE 18: LASER DISCHARGE SECTION



GAS FLOW SYSTEM

FIGURE 19:

LASER BEAM OPTICS



A = Micrometer drive for intra-cavity grating

B = Sapphire Brewster window

BE = Cassegrain beam expander (1:5) f/1.8

C = Differential micrometer adjustments for output reflector

D1 = Pulse energy monitor (Sensors L66-3M thermopile)

D2 = Pulse energy monitor (modified Sensors

C1 thermopile)

G1 = 300 1/mm intra-cavity grating

G2 = 300 1/mm spectrometer grating

L1, L2 = Uncoated germanium lenses

L3 = Uncoated CaF_2 lens (f.l. = 38 cm)

M = Spherical focusing mirror (f.l. = 45 cm)

P = Plane reflector

R = Sapphire flat, coated for 95% reflectance at 45°

S = CaF_2 beam splitter (90% transmission)

U = Gold-coated CaF_2 unstable output reflector (25% output coupling)

FIGURE 20

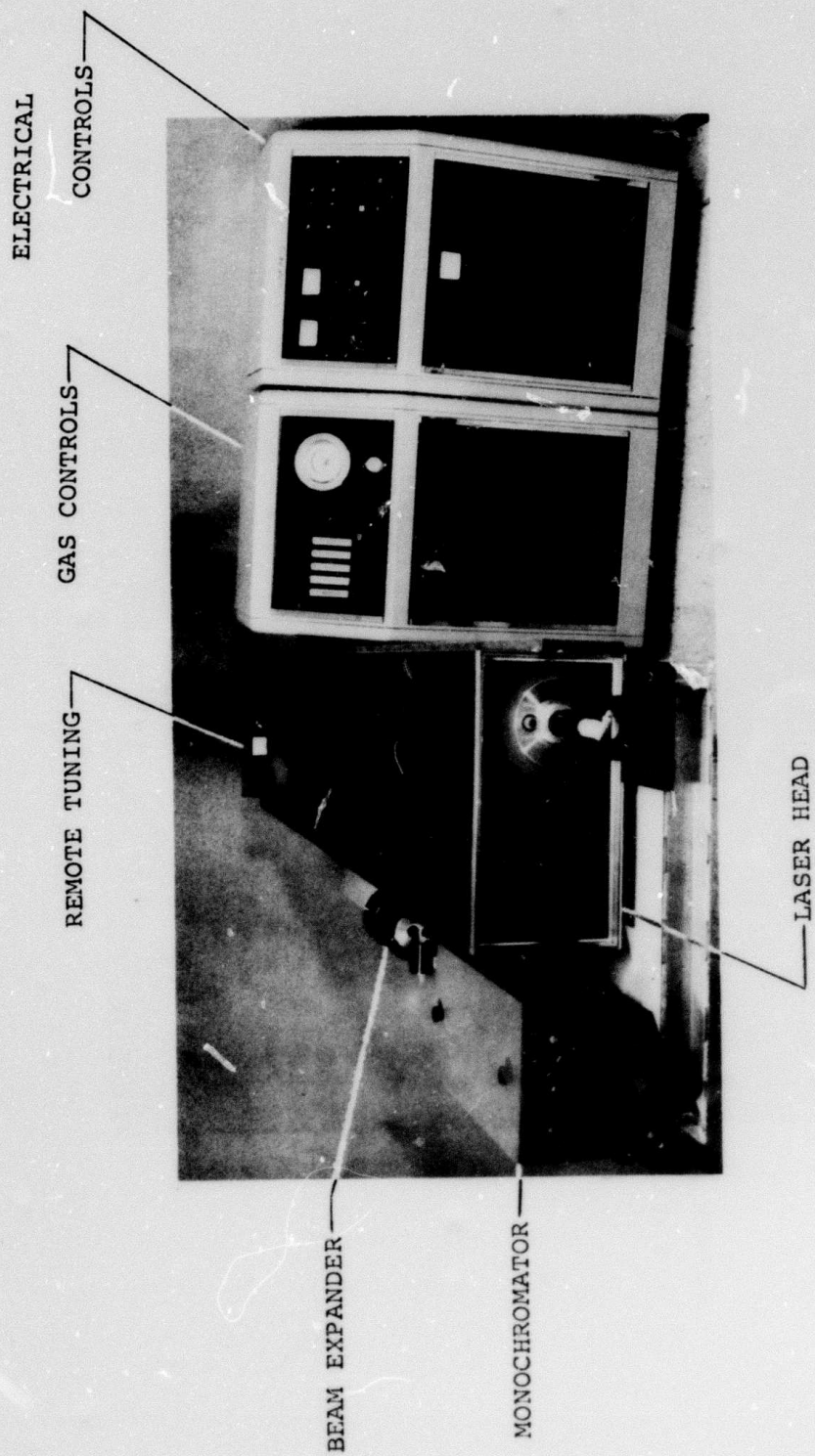


FIGURE 21: HF/DF LASER SYSTEM

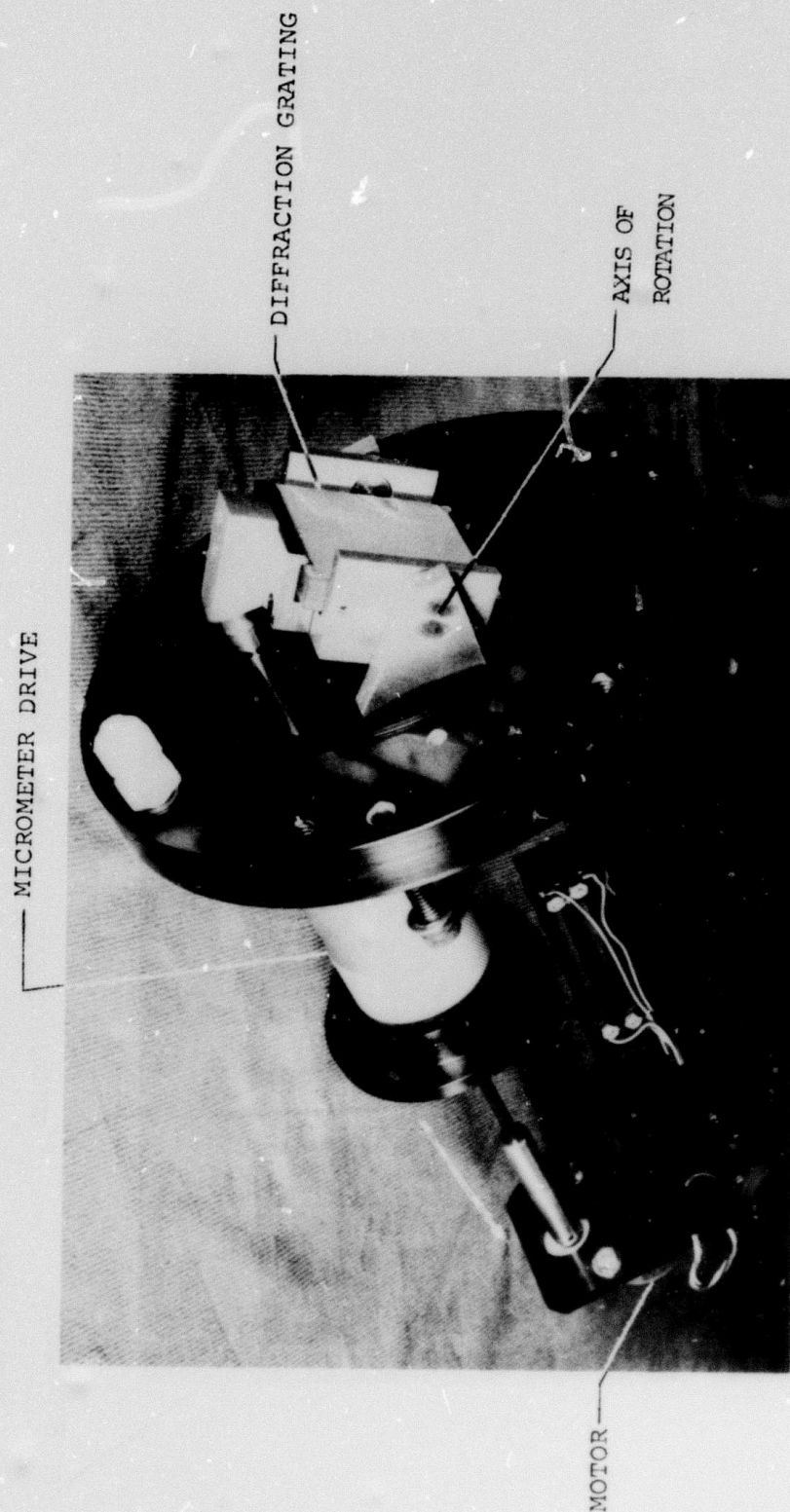
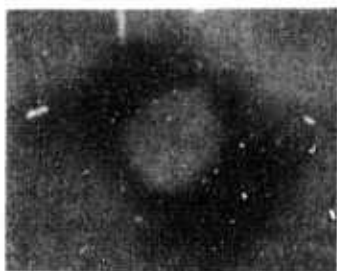
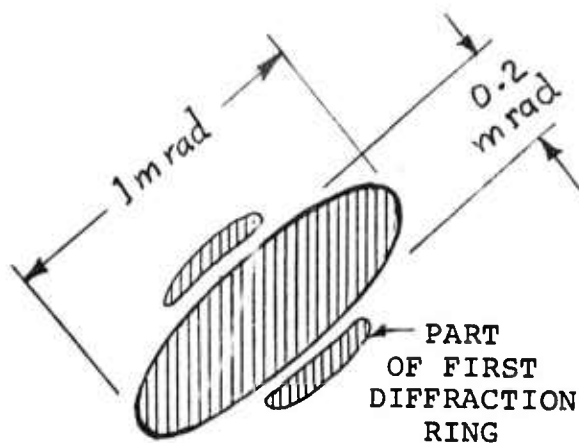


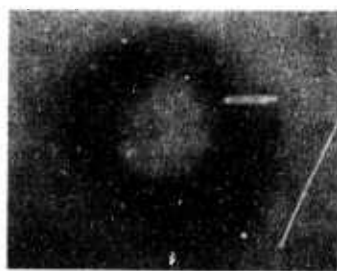
FIGURE 22: GRATING MOUNT AND DRIVE



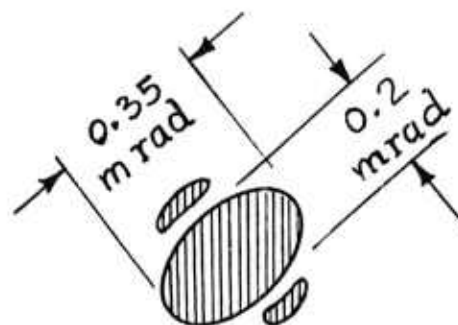
NEAR-FIELD PATTERN
(full scale)
WITH NARROW ELECTRODES



FAR-FIELD PATTERN

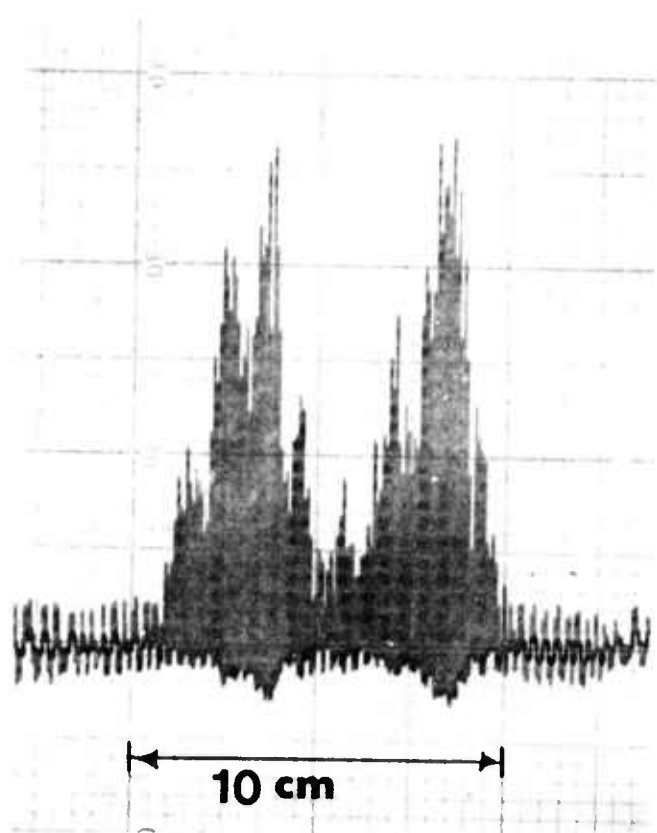


NEAR-FIELD PATTERN
(full scale)
WITH FLATTENED ELECTRODES



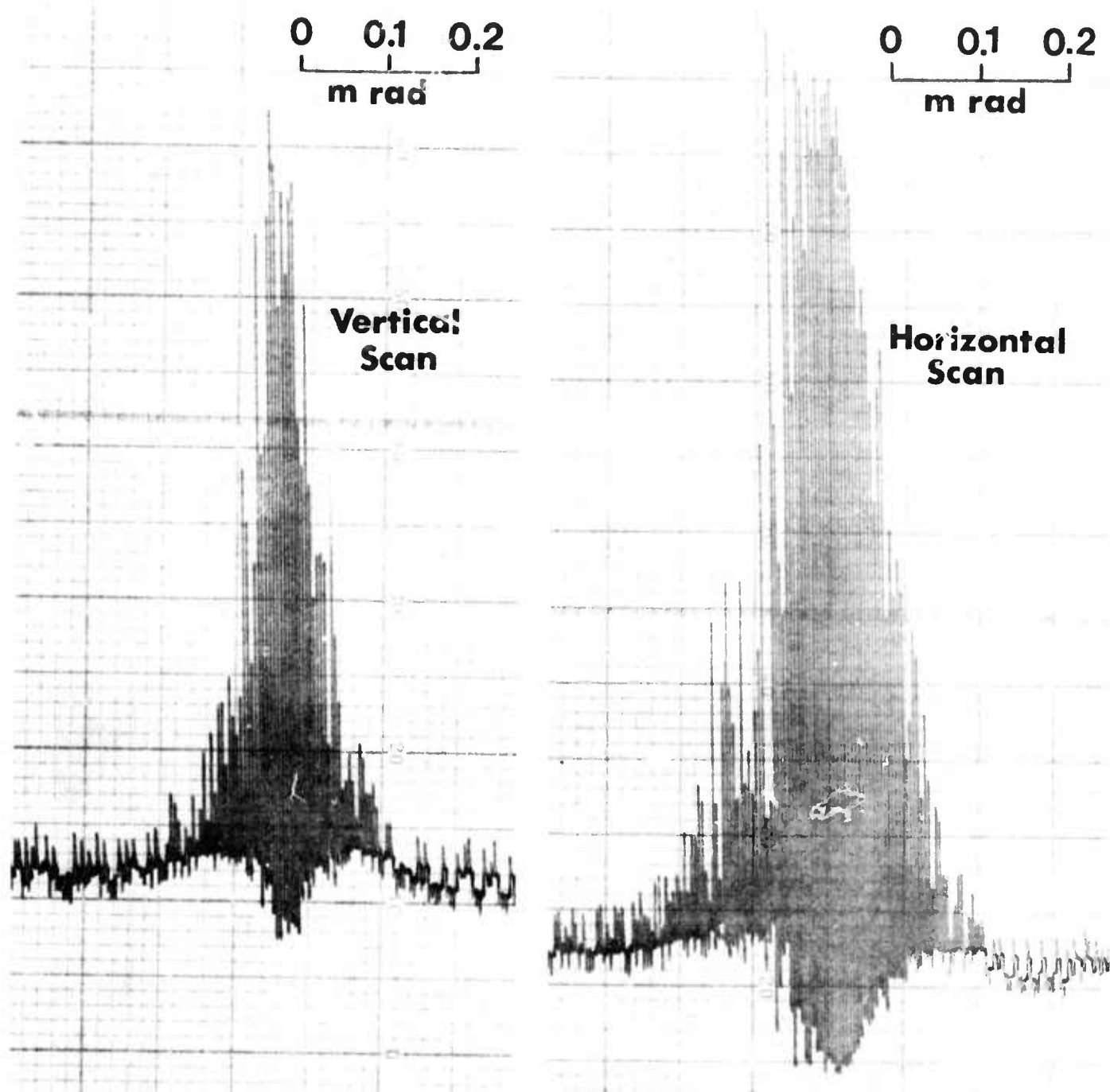
FAR-FIELD PATTERN

FIGURE 23: CROSS-SECTIONS OF THE OUTPUT BEAM FROM THE UNSTABLE CAVITY
FOR TWO DIFFERENT ELECTRODE SHAPES

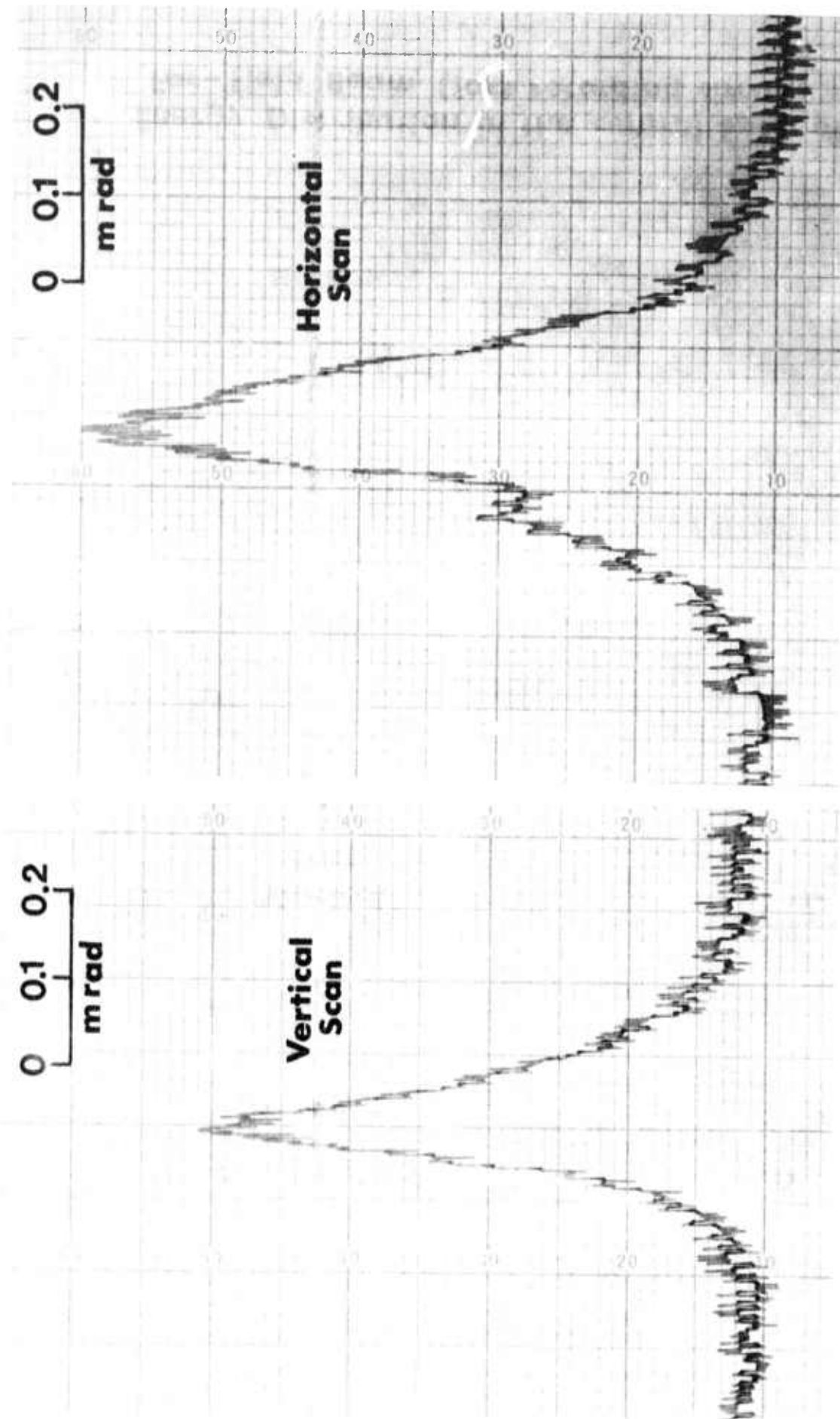


Near-Field Beam Profile 50m from Laser

FIGURE 24



**Energy Distribution in the central Spot of
Far-Field Beam (fast recording circuit)**



Energy Distribution in the Central Spot of Far - Field Beam (integrating circuit)

FIGURE 26

X APPENDIX

SYSTEM SAFETY ANALYSIS

The types of safety hazards encountered during the operation of this laser system (Lumonics HF/DF Laser) may be classified under three headings:

- A. Electric,
- B. Optical, and
- C. Chemical.

Each of these will be discussed separately and in detail below.

Safety aspects have been given due consideration during all design phases of this system, and wherever possible, special safety devices have been incorporated to minimize such hazards. All known hazards have been identified in the instruction manual, and procedures have been written in such a way as to avoid hazardous situations. Hazard levels encountered may be classified as "marginal" (Category II), and could only become "critical" (Category III) through negligence on the part of the operating personnel.

A. ELECTRIC HAZARDS

Molecular excitation of the gas mixture in a pulsed TE-laser is either produced or controlled (as in the present case) by the application of high voltage pulses (up to 40 kV in the system described). All high-voltage (HV) components have been completely enclosed in electrically grounded metal cabinets equipped with safety interlock switches. HV areas and components have been identified by "High-Voltage Warning" signs.

Major HV components are:

1. HV Power Supply in Electric Control Cabinet ,
2. HV Storage and Discharge Circuit inside Laser ,
Cabinet
3. HV Trigger Module in Laser Cabinet .
4. HV Cable between Control Cabinet and Laser
Cabinet is properly shielded and grounded.

The safety interlocks prevent the generation and application of high voltages to any of the system components, if either the laser cabinet cover or the control cabinet door are not closed.

If it is necessary during maintenance procedures to open the electric control console or the laser cabinet, all AC power to the system should first be switched off and the control console be unplugged. Before attempting to perform any work inside the laser cabinet, the terminals of the storage capacitor should first be shorted to ground, as the capacitor is able to store a lethal charge, should some of the electrical connections become loose or "open circuited".

B. OPTICAL HAZARDS

The HF/DF-laser system produces microsecond pulses of radiation in the wavelength range between 2.7 and 4.1 micrometers. Maximum pulse energy of the tuned laser system is less than 100 mJ.

Radiation in this wavelength range is generally absorbed by liquid water, but is partially transmitted by various glasses and plastics.

POSSIBLE EYE DAMAGE:

Retinal damage of the eye cannot occur at these wavelengths, since practically all the energy is absorbed in the cornea. Eye damage would, therefore, be restricted to superficial corneal burns and/or damage resulting from the heating effect due to absorption of the energy within the anterior chamber of the eye. The energy density in the unfocused beam from the laser described herein is too small to cause surface burns, and the amount of energy that can enter the eye is not sufficient to cause any noticeable heating effects. The focused beam, however, has been shown to produce burns on skin tissue.

Whenever there exists the possibility that operating personnel may encounter focused beam reflections from this laser, suitable safety goggles should be worn.

Transmittances measured through various glasses, plastics and goggles placed into the laser beam ($\lambda = 2.79 \mu$) are:

2 mm thick plexiglass	-	5%
6 mm thick "Lexan" polycarbonate	-	<0.1%
Prescription eye glasses	-	40-80%
"Sellstrom" (SM) safety glasses	-	35%
"Laser-Gard" gallium-arsenide neodymium goggles	-	1.5%
"Eastern Safety E28-5" propionate plastic goggles	-	0.2%

Transmittances measured in the untuned multiline HF laser beam ($2.6 - 3.1 \mu$) are:

Prescription eye glasses	- 40-70%
1/4 mm liquid water	- 10%
"Eastern Safety E28-5"	
propionate plastic goggles	- 0.2%

Transmittances measured at a DF wavelength (3.80μ) are:

Prescription eye glasses	- 30-35%
"Eastern Safety E28-5"	
propionate plastic goggles	- $< 0.1\%$

Of the glasses tested, the propionate plastic goggles appear to give the best protection. Note that ordinary eye glasses afford inadequate eye protection against either HF or DF radiation.

C. CHEMICAL HAZARDS

The hazards involved in handling fuel gases and exhaust gases are of a different nature and are discussed in turn.

FUEL GASES:

The fuel gases recommended for this laser are both non-corrosive and non-toxic (H_2 , SF_6 , He, D_2), and no material problems exist with respect to the gas feeding system. The gases are introduced at both ends of the laser cavity to protect the end flanges and optical reflectors from coming in contact with any corrosive reaction products. Similarly, the vacuum gauge and vacuum switch are connected to the gas inlet system.

Sulphur-hexafluoride is considered chemically and physiologically inert, and becomes dangerous only when heated to decomposition.

Hydrogen and deuterium is a colorless gas, which burns with a colorless flame when heated above the ignition temperature in air or oxygen. Spontaneous combustion may occur in the presence of certain catalysts (such as powdered platinum).

Precautions necessary for handling hydrogen are those generally applied to the storage and handling of highly flammable gases. Storage sheds should be well ventilated and should be equipped with hydrogen detectors and alarms.

The amount of hydrogen used in the present system is very small (less than one liter per minute), and the concentration of hydrogen in the lasing mixture is low (less than 5%). Only a small amount of compressed hydrogen needs to be stored near the laser (50 ft³ or less) to minimize the fire hazard.

Furthermore, the amount of hydrogen, which can react with fluorine in the laser cavity is controlled by the number of free fluorine atoms produced in the electrical discharge. Uncontrolled chemical chain reactions (as with $H_2 + F_2$) are not possible with the suggested gas mixture. The quantity of hydrogen which reacts per pulse is again only 5% of the amount introduced, and the heat liberated is negligible.

Although the laser has been thoroughly leak-checked and is not likely to develop leaks under normal operation, frequent leak checks should be performed to prevent uncontrolled amounts of air entering the gas system.

The explosion hazard due to uncontrolled leaks is minimal due to:

1. The low partial pressure of hydrogen in the laser (2 torr),
2. The inhibitive action of the SF_6 diluent,
3. The action of the safety vacuum switch, which will shut off the gas flow and the HF supply, should the pressure in the discharge tube rise above a preset limit.

EXHAUST GASES

Both corrosive and toxic gases are produced in the discharge tube and are pumped out through the vacuum pump. The pump exhaust must therefore be vented outside the laboratory. The exhaust stack should be located well away from populated buildings. In areas where strict pollution standards do not permit dispersion of toxic gases in the atmosphere, the pump exhaust must be chemically scrubbed to remove HF and sulphur compounds before venting into the atmosphere. Hydrogen fluoride may be removed by passing the exhaust through a solid pebble trap of soda-lime or by bubbling the exhaust through a tall column of alkaline solution (e.g. NaOH).

Specific compounds found in the exhaust are:

Undissociated SF_6	> 80% at low pressure operating condition
He	> 90% at high pressure operating condition
HF	< 1%
H_2S	negligible
Decomposition products of SF_6 (SF_n , where $n = 1, 2, 3, 4, 5$)	< 5%
S_2 (as finely divided powder)	Deposited in discharge tube and pump lines.

The actual quantity of HF produced is 5×10^{-5} g-mole/pulse (or 1 milligram/pulse). This number is consistent with the calculated amount based on gas-kinetic and energy considerations, and agrees also with the measured amount in the exhaust obtained by titrating a NaOH solution. Note that almost all the HF passes through the pump and is not trapped in the oil.

A mass spectrometer analysis of the laser exhaust was performed by the Canadian Defence Research Establishment at Valcartier (DREV) and compared with a similar analysis of SF_6 , in order to determine the relative concentrations of SF_5 , SF_4 etc. in the exhaust. No noticeable difference was found, indicating that the concentrations of the decomposition products of SF_6 are small.

The toxicities of the SF_n products are largely unknown and must all be considered as highly toxic.

Cleaning of the discharge tube and changing the pump oil should only be done in well ventilated areas, and direct skin contact with contaminated surfaces should be avoided by wearing disposable plastic gloves.